Bachelor Thesis

DESIGN AND CONSTRUCTION OF AN UPGRADED HYBRID ROCKET

Author:

Sara Esteban Corchado

Director:

Mario Merino Martínez

February 2016

Abstract

Hybrid rockets are a type of chemical space propulsion that is nowadays still in an experimental phase, but that can become one of the most important propulsion technologies due to its advantages with respect to the existing ones.

The present work consist on developing an upgraded hybrid rocket model which has been modified with respect to the existing one in order to obtain better performances and results. The aim of this project is to create a safer model with a safer ignition system as well as a fully redesigned gas-injection and thrust measurement system.

Also, a mathematical one-dimensional model has been implemented in order to predict and study the behavior of the hybrid rocket model to achieve a better comprehension of this topic.

The ultimate purpose of the project is to acquire a deep understanding concerning the space propulsion, concretely the one associated with hybrid rocket propulsion.

Acknowledgments

I would like to take advantage of the following lines to express my gratitude to all the people who has contributed to the success in finishing the present project and who has helped me during these months.

My first mention and special tanks to my director, Mario Merino, for allowing my participation in this project, guiding me in every obstacle that I may have found and for being there at every moment to help me.

Thanks also to my professor Andrea Ianiro for his participation in the project and to Carlos Cobos, without your help and willingness this project would not have been possible.

Final mentions, the last but not the least, for my family, for supporting me always.

To my parents, people to who I owe everything. Thank you for all the sacrifices that you have done with which you have help to bring me where I am now. Thank you for giving me the opportunity to study abroad and four always believing in me and making me realize that I am capable of everything when I thought I couldn't.

I would also like to thank my friends, Raquel, Alba, David, Claudia and specially Irene, for supporting me and always being capable to see the best of me.

Contents

List of Figures

List of Tables

1 Introduction

The Aerospace Engineering department at *Universidad Carlos III de Madrid* has a laboratory model of an hybrid rocket engine, which is mainly used for the better understanding of the space propulsion systems during the laboratory sessions of the last year BSc course 'Rocket Motors' which belongs to Aerospace Engineering Degree.

The aim of this project was to upgrade and improve the existing hybrid rocket to make it easier to control and to obtain more accurate results, as well as establishing a one-dimensional mathematical model with which the behavior of the rocket can be studied. In order to do so, some modifications were expected:

- Install an upgraded system to remotely control the gases flowing into the rocket's combustion chamber.
- To provide a safer and simpler method to ignite the hybrid propulsion system.
- To obtain more accurate results when measuring the thrust provided by the rocket.

To reach the desired objectives of the project, some modifications of the existing model had to be made:

- It was necessary to redesign and build some existing parts and to create new ones.
- A completely new gas installation in the laboratory.
- Completely new ignition system using a glow plug instead of a match, which made the experiment safer.
- Improved thrust measurement system by introducing a load cell in the model.

The main purpose of upgrading the previous model was to make a new design more accessible and safer, as well as providing a model that allows a wide range of combinations and results by means of varying the proportion in which gases are mixed for combustion.

Apart from the experimental measurements, it is interesting to develop a mathematical model to predict the behavior of the combustion process under different conditions. It consists of a one-dimensional model that analyzes the equations of continuity, momentum and energy so that the variation of several properties such as the velocity, the pressure, the density and the temperature can be established along the axial direction as the flow passes through the duct and the nozzle.

The variation of these magnitudes is about to be analyzed for several cases: taking into account only the variation of the area and considering the effects of the friction forces, the addition of mass from the walls and the addition of heat.

The tool that is going to be used to determine the performance of the model is Matlab.

1.1 The hybrid rocket at UC3M

A prototype of an hybrid rocket was designed and built at University Carlos III Madrid with the purpose of complementing and upgrading the teaching methods for the Degree in Aerospace Engineering. The main objective was to create an experiment with which the principles and theories of space propulsion could be explained to the students.

The first design was based on the model developed by the Aeronautics and Aerospace Department at Massachusetts Institute of Technology and it was carried out by the professor Manuel Martinez Seisdedos together with some of the Aerospace Engineering department professors, students and technicians.

All the parts of the propulsion system were designed with Solid Edge according to some previously defined parameters such as:

- The thrust was limited to around 20 N and a convergent nozzle was going to be used.
- The solid fuel used was poly (methyl methacrylate) and the gaseous oxidizer was oxygen.
- The design had to be easily accessible, safe and open to changes in the design.

As it was mentioned before, the new model comprises an upgraded ignition system, a new thrust measurement system and a new movable structure in which the rocket is placed, that allows to obtain better measures from the load cell.

With this new model, further experiments can be carried out by varying some conditions like the amount of gases injected or its proportion and therefore it will let us to acquire a better knowledge concerning its behavior.

1.2 Objectives of this project

The aim of this project is to redesign the existing prototype in order to improve its performance and to eliminate the existing weaknesses.

The main objective is to improve the safety when igniting the rocket by creating a system in which three different gases could be remotely injected and ignition is achieved by means of applying voltage to a small glow-plug installed in the upstream part of the rocket. To do so, it is necessary to design some new parts of the rocket and to modify the existing ones to adapt the model to our new necessities.

Thanks to this, the previous method in which the rocket was ignited by introducing a match through the exit orifice is eliminated. This way was much simpler but also dangerous, since it was necessary a person standing in the ignition room, with risk of a fire or explosion that could cause several injuries.

Apart from changing the ignition method, as it was mentioned before, a new gas installation is needed in the laboratory with which the proportion of gases can be controlled more accurately from a remote system outside the essays room.

The last important improvement is related to the thrust measurement system. In this new model it will be made with a load cell installed in the front part of the rocket that will provide a value of the thrust achieved when the rocket is ignited and it presses the cell due to the action-reaction principle.

The new model is supposed to allow us to measure a wider range of magnitudes and to operate in different conditions depending on the mass flow of the injected gases, the proportion in which they can be injected or the length of the propellant tube.

As it was aforementioned in the introduction, apart from the experimental part, a one-dimensional mathematical model studying the behavior of the rocket under different conditions will be implemented in Matlab. This part of the project is interesting since the behavior of the rocket can be in some way anticipated and it will make possible to compare the experimental results with the theoretical ones obtained with the model.

However, the model is not going to predict completely the real performance of the thruster since the theoretical model is going to be assumed as one-dimensional to simplify the calculations. Nevertheless, it is going to give us feasible predictions and it will allow us to get a better understanding of the combustion process and how the flow behaves under different conditions and assumptions.

1.3 Structure of this report

The structure of this report will include several parts. Section 2 will comprise the theoretical background of the space propulsion, with the explanation of the main characteristics, configurations, advantages and disadvantages, as well as some important definitions related to it such as the thrust, the specific and total impulse, the effective exhaust velocity and the characteristic velocity.

Right after this, in Section 3 all the process related to the design of the experimental rocket will be explained in detail. This part will comprise the design requirements, the geometry of the pieces and its machining, the rocket assembly and the explanation of the current thrust measurement system.

This part will be immediately followed by a description of the combustion reaction that takes place inside the rocket when it is fired, the description of the first firing and the test results along with the problems and possible solutions found in the experiment.

Straightaway, Section 5 will comprise everything regarding the mathematical model. First of all, a theoretical background explaining the different cases that can be found for a one-dimensional flow is going to be exposed, and it is going to be followed by the assumptions, hypotheses and procedures made in order to develop the model associated to this project. The results of the analytic part are going to be shown at the end of this section.

The last part will consist of a study of the future work and modifications that can be done to the hybrid rocket, an analysis of the work done and a preview of the future work that can be done concerning this project.

Furthermore, the project includes some Annexes that comprise the combustion reaction of PMMA explained in detail, the plans of all the parts of the rocket and a user guide of the load cell used in the project.

2 Hybrid rockets generalities

Rocket propulsion can be divided into two main sub-categories: chemical propulsion rockets and nuclear propulsion rockets. While the chemical ones obtain their thrust from the reaction of chemical propellants at high pressure, nuclear systems work by transferring heat from the reactor to the working fluid, which is expanded through the nozzle. Among the nuclear propulsion systems, we can mainly differentiate between rockets working with fission or fusion reactors.

Chemical rocket propulsion systems can be classified depending on the method by which they produce thrust, by the type of vehicle, the size, the type of propellant or by the kind of source of energy that they use, among others.

Figure 1: Rocket launching.

By observing the kind of propellant that is used, we can differentiate between liquid propellant rockets, solid propellant rockets and hybrid propellant rockets. This last one is going to be the one studied in detail for the present project.

Rocket propulsion systems, in general, obtain the thrust by means of ejecting the propellant at high speeds. To reach supersonic velocities, the flow is made to pass through a convergent-divergent nozzle that accelerates the fluid. As the flow passes through the nozzle, there is an important drop in pressure and temperature and its thermal energy is converted into kinetic energy.

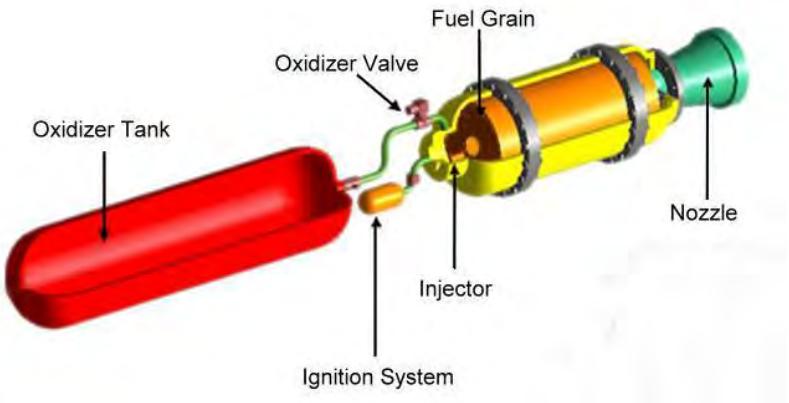

Figure 2: General scheme of a Hybrid Rocket

The rocket motor is one the most powerful motors ever built, and its relation weight-to-thrust is also the biggest one up to date. It is the most suitable for space vehicles since these missions require large amounts of thrust in order to reach the necessary velocity to exit the atmosphere.

Hybrid motors are propulsion systems in which one component of the propellant is in liquid phase, which is typically the oxidizer, while the other one, the reducer or fuel, is stored in solid phase. In hybrid motors, the way in which the liquid propellant -oxidizer- is pressurized is not a critical element, so that there is no need for a very complex injection system, which is traduced in less valves and plumbing.

In hybrid motors, the liquid oxidizer can be directly injected in the combustion chamber, where it mixes directly with fuel, or in a pre-combustion or vaporization chamber upstream of the solid fuel grain. To ensure that the solid and liquid propellant components react completely, usually a post-combustion chamber is placed downstream, right before the nozzle exit. In order to accomplish the reaction, the fuel grain is made with a high number of axial combustion ports that evaporate more easily to react with the liquid oxidizer injected.

2.1 Applications of hybrid rockets and propellants used

Hybrid propulsion is very suitable for missions that require throttling or shut-down and restart commands, like long duration missions requiring nontoxic propellants or infrastructure operations needing non-self-deflagrating systems. The technology of hybrid rockets takes advantage from the development and improvements achieves for solid and liquid rockets: they avoid the difficulty of dealing with the fuel configuration in solid rockets and the mechanical complexity of liquid propellant rockets.

Some examples of applications of hybrid rockets are:

- Target missiles and low-cost tactical missile applications.[37]
- Space motors. The characteristics of hybrid rockets make them suitable for for satellite maneuvering or to adjust the exact velocity of a space vehicle.
- Reinforcement for the main thrust in the space vehicles launching.

Early hybrid rockets were made for tactical missile applications [37]. Some other developments were focused on upper-stage motors that required high-energy systems. Recently, all the efforts have been focused on booster prototypes for space launching applications. Nevertheless, hybrid rockets are still in an experimental phase, and up to date this kind of propulsion system has not been chosen for big production applications.
Regarding the propellant used, many investigations have been made using a wide range of oxidizers and fuels:

- High-energy combinations include the use of oxidizers such as fluorine/liquid oxygen mixtures [37] or chlorine/fluorine compounds used together with high energy fuels like lithium, aluminum or beryllium mixed with a suitable polymeric binder [26]. These high-energy propellants deliver specific impulses in the range from 350 to 380 seconds and combustion efficiencies around 95%.
- A lower energy propellant system, but more practical, is the one using a combination of a 90% of hydrogen peroxide as oxidizer with hydroxyl-terminated polybutadiente (HTPB) fuel (this component is used in solid propulsion systems as the binder to make firm the propellant matrix) [37]. These combination is quite advantageous,

since the hydrogen peroxide is relatively inexpensive and can be stored for long periods of time and the HTPB processes easily, is low cost and does not self-deflagrate.

- For large hybrid booster applications HTPB is used again as the fuel while the oxidizer is liquid oxygen. This combination provides a nontoxic and almost smoke-free exhaust gases.

For some applications powdered aluminum was added to the fuel, provided that an smoke exhaust is not a drawback.The aluminum rises the combustion temperature while decreasing the stoichiometric mixture ratio and increasing the density of the fuel.
Up-to-date, all the work developed in hybrid propulsion systems has been towards achieving motors with a thrust level around 1,112,000 N.

The procedure to ignite the rocket is the following: the hybrid fuel grain is ignited with a source of heat. The heat provided starts the evaporation of the solid propellant that turns into a flame once the liquid oxidizer is injected. Ignition is usually completed by injecting an hypergolic fluid that spreads the flame through the motor[1].

Small models of hybrid motors like the ones used for laboratory experiments are usually ignited electrically, making a current pass through a resistor located in the combustion port or using a propane or hydrogen ignition system. The last mentioned is the one to be used in the upgraded hybrid rocket at UC3M.

2.2 Main advantages and disadvantages

In first place, the advantages of this kind of motors will be exposed:

- The main advantage of these motors is their safety compared to solid or liquid propellant rockets. Unlike the others, in hybrid rockets the reaction only takes place once the two propellant are brought together, so that the rocket can be stopped or restarted when necessary[2].

- The propellant is inert, so that the risk of self-ignition due to vibrations or collisions during fabrication, storage or operation is minimized[3].

- The main characteristic of these motors is their capability of working over a wide range of conditions since many parameters can be changed on demand:

  - The combination oxidizer-propellant. With a hybrid rocket we can access to a wider range of combinations.

  - The shut-down or restart capability: the hypergolic ignition can be achieved too when there is an spontaneous ignition when both the fuel and the oxidizer are brought together.

  - The chamber pressure can be varied, which is determining in the nozzle actuation and has a low influence in the evaporation-combustion process.

- A higher specific impulse is achieved with hybrid rockets[1].

- These motors are very resistant thanks to its simple configuration and low working temperatures and due to the imperfections allowed by the solid propellant in its construction, that barely affect to its functioning.

- They are not very sensible to the ambient pressure, just like liquid propellant rockets, so that the change in ambient temperature has a very low impact in the chamber pressure, so that the are more easily designed[37].

- Low environmental impact with a good propulsive efficiency (the best one in thermochemistry).

- Low manufacturing cost due to the non-extremely exigent design conditions and the wide range of propellants and oxidizers that can be used, which allows the possibility of taking more economical materials as well as the avoidance of problems related to delicate feeding systems or chamber pressure and temperature controlling. This is probably the best advantage of hybrid propulsion systems[1].

However, this type of propulsion has noticeable disadvantages that delay their development, so that up to date only some prototypes have been tested. The principal drawbacks are:

- Low fuel vaporizing speed, which provokes the impossibility of the rocket of producing a constant thrust. This makes that the mixture ratio and, in consequence, the specific impulse will change during steady-state operation and throttling.[4]
- Low volumetric density of the fuel. As a consequence of the low vaporizing speed, a high fuel surface area is required to obtain the desired thrust. This is achieved by means of the combustion ports, which leads to a lower density referred to the volume that the fuel occupies in the motor.[2]
- Low fuel grain efficiency compared to other propulsion systems. This is due to the fact that in hybrid rockets combustion is achieved by means of the diffusion flame and not by the premixing conditions, such as in liquid or gaseous propellant rockets. This reduces notably the combustion efficiency with a loss of approximately 1-2% higher than in solid or liquid rockets.[5]
- Hybrid rockets deliver a relatively lower specific impulse compared to solid propellant rockets.
- Some fuel is retained in the combustion chamber (slivers) and at the last part of the rocket, at the end of burn, causing a decrease in the motor mass fraction.[1]
- Unproven propulsion system feasibility at large scale.

2.3 Fuel grain configuration and performance analysis

The performance of this type of propulsion system is highly dependent on the achieved degree of mixing in the combustion chamber. Hybrid rocket's fuel regression rate[1] is usually less than one-third that of solid propellant rockets. For this reason, multiple perforations, called combustion ports are made in the solid propellant so that the fuel surface area is increased.

These ports allow to rise the combustion efficiency of the rocket as a consequence of the turbulent background in which unreacted fuel and oxidizer are mixed in the downstream part of the rocket.

The number of combustion ports in the fuel grain is set depending on the desired thrust level.

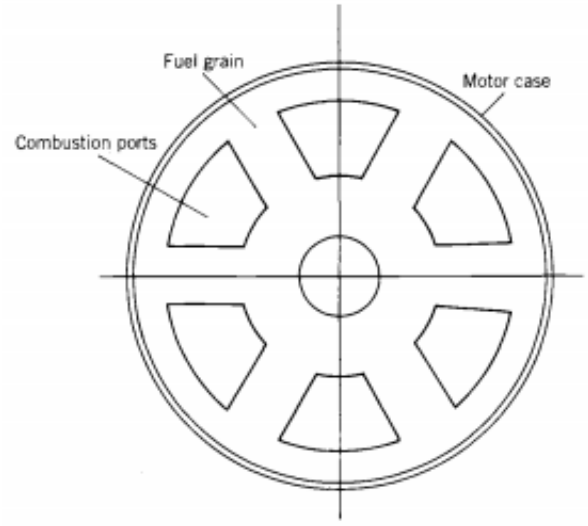

Figure 3: Cross section of a typical high-thrust hybrid fuel grain with multiple combustion ports

[1]The regression rate is the velocity at which the surface of the solid propellant is consumed because of its vaporization due to the combustion process. It is largely dependent on the pressure and it is exponentially proportional to the temperature. [1]

The characteristic velocity of the rocket is settled by determining an specific oxidizer-to-fuel ratio. Consequently, the mass flow rate is established once the previous values (characteristic velocity and mixture ratio) are known, together with the total surface area and the regression rate of the fuel.

The performance of hybrid rockets can be considered as a combination of that of solid and liquid propellant rockets, with the main difference being the mechanism by which the solid propellant is ignited and the fuel regression rate.

The main problem associated with the combustion of the solid propellant are the *slivers*, which are remains of unburned propellant. They appear at the periphery of the grain and their main disadvantage associated to them is the decrease of the propellant mass fraction and the mass ratio of the space vehicle. [1]

Since the solid component of a hybrid rocket does not include oxidizer in its composition, the regression rate is quite different.
In a solid propellant rocket, the combustion of theis heterogeneous and it can be defined by the following relation

$$\dot{r} = ap_1^n \tag{1}$$

where a and n are empirical coefficients obtained experimentally.

The selection of the components conforming the fuel grain is critical to achieve a desired regression rate, since it is a function of the heat of gasification of the fuel, which, in other words is the energy required to evaporate the solid fuel grain.

Considering an energy balance at the surface, the subsequent expression is derived for the regression rate in a hybrid rocket:

$$\dot{r} = K\frac{G^{0.8}}{\rho_f}\left(\frac{\mu}{x}\right)^{0.2}\beta^{0.23} \tag{2}$$

where K is a constant, G is the free stream propellant mass velocity at a given axial location x, ρ_f is the density of the solid propellant, μ is the viscosity of the combustion gas and β is the non-dimensional fuel mass flux. The last parameter, β is similar to the

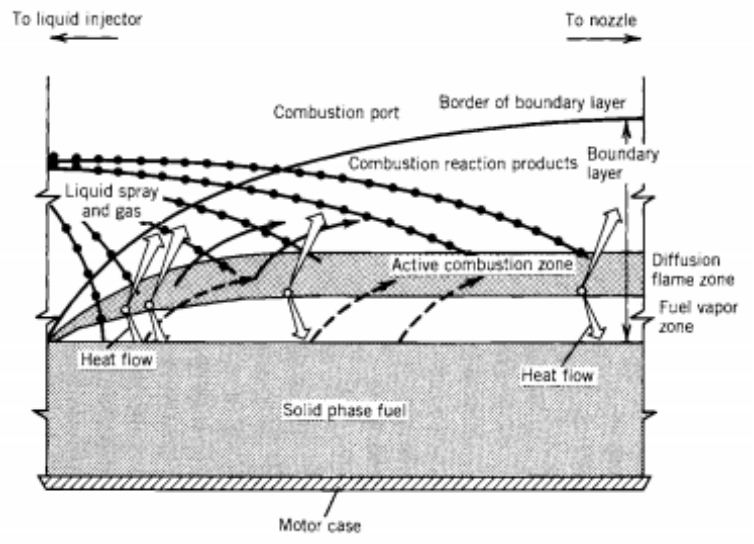

Figure 4: Scheme of the combustion process and heat transfer at the combustion port wall

constant G but it takes into account the evaporation of the fuel and it is evaluated at the fuel surface. [1]

As it can be deduced from the expression, the regression rate is highly dependent on the value of G but not on the axial location. Since x is in the denominator it can be anticipated that the regression rate will decrease as we move forward in the axial direction. In a first approximation, it can be appreciated too that it is no longer dependent on the chamber pressure.

However, this expression is usually simplified with the purpose of making an easier preliminary design, taking into account the effects of β, x, ρ_f and μ into a parameter a, which leads into the following expression

$$\dot{r} = aG_0^n \tag{3}$$

where G_0 is the oxidizer mass flux per unit area. With this definition it is possible to characterize in a simple and approximate manner the desired combination of fuel and oxidizer.

2.4 Definitions and fundamentals of space propulsion

As it was mentioned before, propulsion in space vehicles is achieved by accelerating the body by means of applying a force to it. This force is a resultant of ejecting matter -propellant- at high velocity.

However, rocket propulsion is not a fundamental subject, so that there are no scientific laws and theories specially applied to it that can explain in detail its behavior. Its basic principles and fundamentals are based on thermodynamic, chemistry and mechanic laws.

Thrust

It is the force produced by the propulsion system of a vehicle, or, in other words, the force produced when the propellant is ejected at high velocity through the exhaust nozzle. Because of the principle of action-reaction, the momentum of the exit gases has the same modulus as the one received by the rocket.

The momentum is defined as the product of the mass by the velocity. In rocket motors low quantities of gases are ejected at high velocity to obtain this effect. It can be defined by the following relation:

$$F = \dot{m}v_2 + (p_2 - p_3)A_2 \tag{4}$$

where $\dot{m}$ is the mass flow rate, v_2 is the velocity with which the gas exits the rocket, p_2 is the pressure at the exit of the nozzle, p_3 is the atmospheric pressure and A_2 is the area of the cross-section at the exit of the nozzle. [24, 25]

As it can be seen in equation (4), the thrust is a result of two different contributions. The first term of the expression is the so-called *momentum thrust*, which is the product of the mass flow by the velocity. The second term is the *pressure thrust*, and it is the product of the exit area of the nozzle and the pressure difference between the exhaust and the ambient pressure.

The notation used is described in the following scheme:

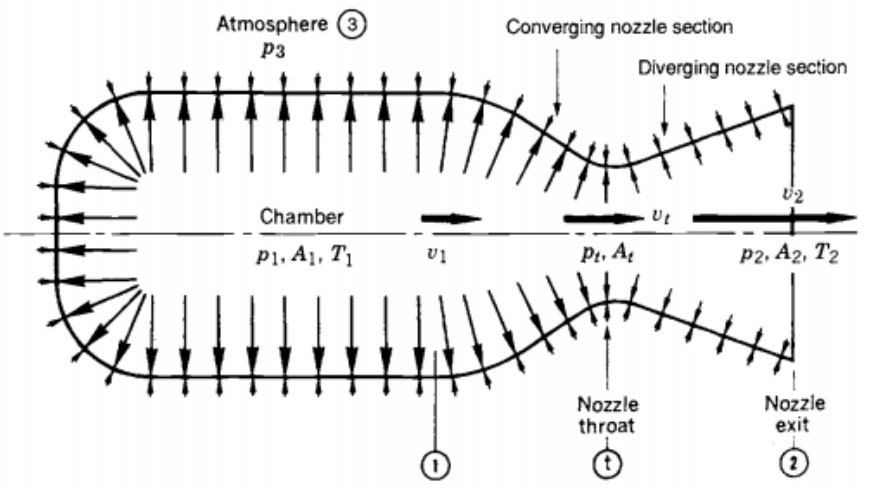

Figure 5: Scheme of an isentropic nozzle. Notation: 0 - Stagnation conditions, 1 - Chamber conditions, t - Throat conditions, 2 - Exit conditions, 3 - Ambient conditions.

Rockets are usually design to give an exit pressure equal or higher than the ambient pressure to avoid a negative contribution to the thrust.
A nozzle is said to be working in optimum conditions or *matched* when the exit and ambient pressures have the same value, $p_2 = p_3$.

Thrust Coefficient, C_F

The thrust coefficient is a non- dimensional parameter and it can be described with the following relations:

$$C_F = \frac{F}{A_t p_1} \tag{5}$$

where A_t is the area of the throat section and p_1 is the pressure inside the chamber.

$$C_F = \sqrt{\frac{2\kappa^2}{\kappa - 1}\left(\frac{2}{\kappa + 1}\right)^{(\kappa+1)/(\kappa-1)}\left(1 - \left(\frac{p_2}{p_1}\right)^{(\kappa-1)/\kappa}\right)} + \frac{p_2 - p_3}{p_1}\frac{A_2}{A_t} \tag{6}$$

Total Impulse, I_t

The *total impulse* is the parameter that gives us the distance that the rocket can cover or the maximum height that it can reach. It is defined as the integral of the thrust over the burning time:

$$I_t = \int_0^t F dt \tag{7}$$

However, this value is not very useful in its own, since two rockets having the same total impulse can present totally different performances.

Effective exhaust velocity, c

In a rocket nozzle the exhaust velocity is not uniform at the exit and it is difficult to measure so, in a first approximation, for a one-dimensional analysis it is convenient to estimate a uniform exit velocity, c. It is the so-called *effective exhaust velocity*, and it is equivalent to the speed at which the propellant is ejected through the nozzle exit. It can be defined as:

$$c = \frac{F}{\dot{m}} \tag{8}$$

Characteristic velocity, c^*

The characteristic velocity, represented as c^* is given by the following expression:

$$c^* = \frac{p_1 A_t}{\dot{m}} \tag{9}$$

It is used to compare the relative efficiency between different designs of chemical rockets. It is highly related to the combustion efficiency and it is independent from the nozzle configuration.

Specific Impulse, I_{sp}

The *specific impulse* is defined as the total impulse per unit mass of fuel. It is measured in seconds and it is an important quantity to define the performance of a rocket. It can be computed with the following expression:

$$I_{sp} = \frac{F}{\dot{m} g_0} = \frac{c}{g_0} \tag{10}$$

The biggest I_{sp}, the better performance.
The specific impulse can also be used to predict the rocket motion with the Tsilkovsky equation:

$$\Delta V = g_0 I_{sp} \ln\left(\frac{M_{initial}}{M_{final}}\right) \tag{11}$$

With this equation, the performance that a rocket must fulfill to undertake any maneuver can be known. However, it does not take into account neither the gravity field losses nor the drag losses due to the atmosphere resistance. Also, it considers that the I_{sp} is constant.[1]

3 Hybrid rocket design and construction

3.1 Design requirements

Although it was not necessary, it was decided to rebuild again all the existing parts of the rocket to ensure that the new parts would fit perfectly with the existing design.
As it was mentioned before, the project is based on an already existing hybrid rocket which, in turn, is a model based on a prototype created by the Aeronautics and Aerospace Department at Massachusetts Institute of Technology.

However, the existing model needed some improvements with respect to the original design to make it safer and more accessible.

The main requirements that the rocket has to accomplish are:

- It has to allow the injection of three different gases in the primary chamber: pure oxygen, propane, and nitrogen. The oxygen is the responsible for accomplishing the combustion process when it is brought in contact with the solid propellant. The propane is mainly used to produce the spark that will ignite the gases and will lead to the start of the combustion. The last one, nitrogen, is mainly needed to extinguish the flame in the case of a fire and to clean the channel from the oxygen excesses.
- The rocket must be able of being remotely ignited by means of applying voltage to a glow plug .
- It must offer a measurement of the thrust produced by the rocket.
- The architecture of the rocket must be done in a way that all the parts can be easily re-designed and replaced by new parts according the needs of the experiment.
- The safety must be improved with respect to the previous model.

3.2 Description and schematics of parts and components

As it was already said, our design is modular, composed by many different small parts that can be changed when needed to meet the desired requirements. In the picture below, an schematic of the whole rocket is shown, in which the three different blocks are clearly defined:

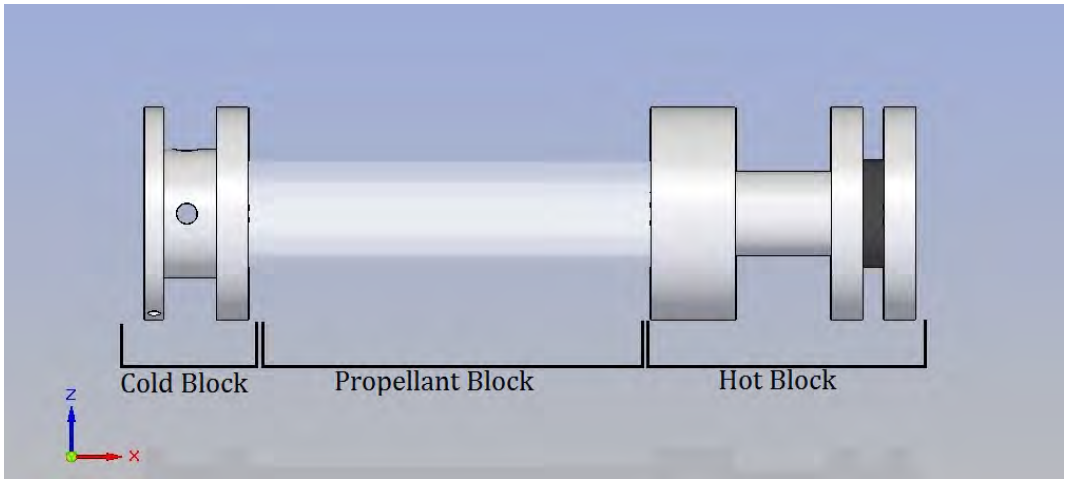

Figure 6: Computer-Aided Design CAD of the Rocket

In the following pages the design of each block and part of the rocket will be explained in detail, as well as the reason for its geometry and its main function. The metallic pieces are enumerated from 1 to 6 as it is shown below:

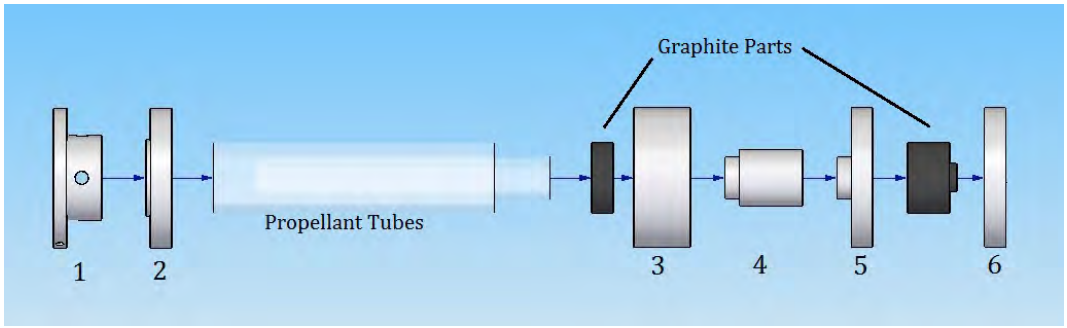

Figure 7: Scheme of the Rocket

In this hybrid rocket model three different parts can be clearly differentiated, two metal block separated by the propellant block:

- Cold block

  The original design consisted of a single metal block with a calibrated orifice[2] in its extreme by which the gaseous oxidizer is introduced.

  This is the part that has been more dramatically changed with respect to the previous model. Instead of having just one solid part with an orifice in its end, the new design will be composed of two parts forming a small combustion chamber in which the gases are well mixed before the combustion.

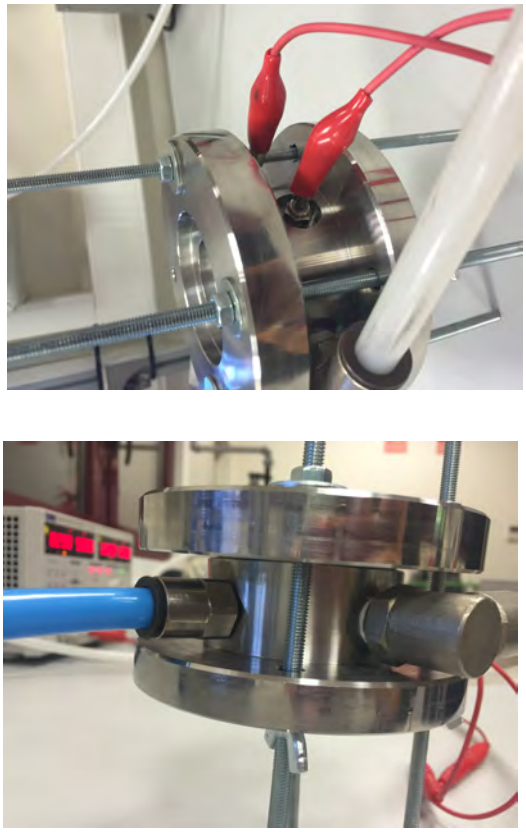

Figure 8: Cold Block.

[2]The calibrated orifice makes possible to measure the mass flow of oxygen that is flowing into the system.

This block has four different orifices: three of them for the injection of the gases (propane, oxygen and nitrogen) and the fourth will serve as the fastening of the glow plug that will be used to start the combustion process.

To make the fastening of the glow plug, it was necessary to acquire the equivalent thread to make the perforation in the inox piece. The glow plug is introduced in this orifice until a tiny part of its surface stands out of the wall surface so that, when it is ignited the gases can be in contact with it to make the ignition possible.

As it is shown in the picture, two cables are connected to the thruster. One of them is connected to the glow plug terminal and the other to the rocket itself (the rocket acts as ground). Both cables are also connected to a voltage source. Therefore, when the source is powered on, the voltage is made to pass through the cables and the glow plug is heated.

- Propellant block

  It consists of two tubes of poly(methyl methacrylate) one placed inside the other with a central hole to allow the flow of the oxidizer inside it.
  When the internal surface of the inner bar is vaporized due to the high temperature coming from the flame created in the pre-combustion chamber and it mixes with the oxidizer the combustion process takes place, generating a plume.

- Hot block

  It is the part in which the post-combustion takes place. It is made up of four metallic pieces and two graphite parts. The last graphite piece acts as a convergent nozzle by which the exhaust gases exit the rocket. The geometry and function of all the pieces will be explained in detail right below.

The rocket is made up of several independent parts to allow different experiments changing some parameters of the rocket such as the length of the post-combustion part, the length of the propellant section (PMMA tubes) and to make it easier to change its geometry for future improvements. Each part individually is going to be described here under:

Cold Block

Also denoted as the injector head. The upper part of the rocket model is made up of two metallic parts.

This corresponds to the part by which the gases are introduced; the two parts, wen brought together, create a small combustion chamber where gases are injected and ignited with the glow plug.

In this block the main combustion process (the one that occurs when oxygen and PMMA react) does not take place and it is not crossed by hot gases at any moment. It serves as an ignition chamber where the initial flame is created.

The reason for building the pieces with stainless steel is because it is more resistant to high temperatures and, since the rocket is in contact with oxygen, an oxidation-resistant material was needed.

Therefore, this piece, as well as almost all the rest of the rocket pieces, are made of stainless steel.

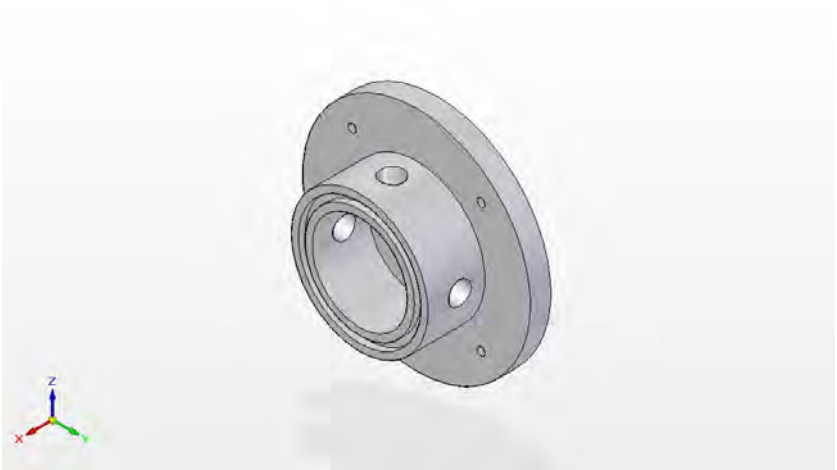

Figure 9: Stainless Piece 1

The previous CAD picture shows the first part of the rocket. As it can be observed it contains four different holes: the one in the axial direction of the flow is the orifice by which the oxygen is injected into the combustion chamber, while the other three orifices are for the propane, the nitrogen and the last one serves to hold the glow plug.

Oxygen is injected in an axial direction so that its injecting velocity helps in propagating the combustion process to the rocket.
Propane is injected in a perpendicular way to oxygen so that both gases are well mixed before igniting.
Nitrogen serves as a flame extinguisher at the end of the firing and cleans the rocket flow path from residual oxygen and propane to avoid fires when the rocket is disassembled.

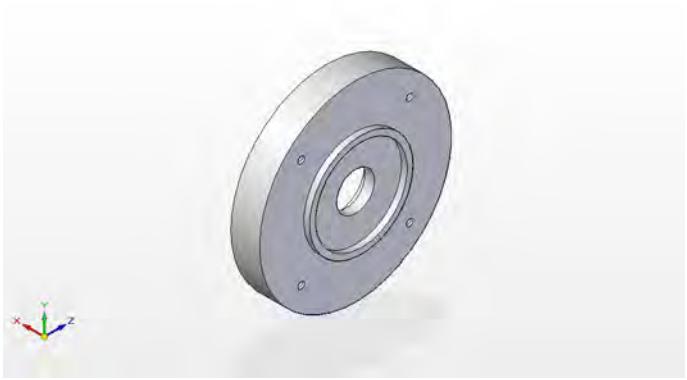

(a) Front view

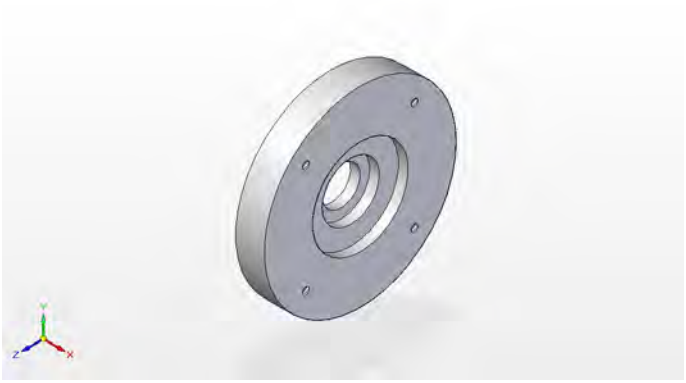

(b) Back view

Figure 10: Stainless Piece 2

The second piece is coupled to the first one by means of introducing the annular protrusion into the groove of the first part, creating the combustion chamber.
This part has a big orifice in its face by which the ignited gases exit the cold block to enter into the propellant block.
As it can be appreciated in the back view of the part, it has two heights of different diameters in which the propellant tubes are introduced.

Propellant Block

The propellant of the rocket consists of tho tubes of PMMA with different diameters placed one inside the other but without contact between them.
The main reason for using two bars is the safety since, in the case of an explosion or fragmentation of the inner tube, the external one will keep the pieces from harming its surroundings.
The PMMA or poly methyl methacrylate, also called acrylic or most commonly *Plexiglas* is a transparent thermoplastic often used as an alternative to glass.

Figure 11: Plexiglas tube

The reason for using it as a solid propellant is because of its favorable properties:

- Transparency
- High impact resistance
- Light material: its density is $1190 Kg/m^3$
- Easy combustion
- Non-toxic exhaust gases
- Easily machined and shaping

The dimensions of the tubes used in the rocket are the following:

Tube	Internal Diameter	External Diameter	Length
Inner	20 mm	30 mm	210 mm
Outer	40 mm	50 mm	200 mm

Table 1: Dimensions of Combustion Port

The dimensions of the tubes have been designed following the ones of the previous model. However, the length of the tubes can be changed to see the relation between the propellant length and the thrust produced by the rocket.

Its chemical properties are shown in the following table

Chemical Composition	$(C_5O_2H_8)_n$
Melting Point	433 K
Heat of Reaction	24.89 MJ/Kg
Adiabatic Flame Temperature	2200 °C

Table 2: Chemical Properties of PMMA [14, 40]

Hot Block

The hot block is placed right after the propellant block and it consists of 6 different parts, being four of them made of stainless steel and the other two made of graphite.

In first place, a graphite piece is found. It is a mouthpiece placed immediately after the combustion port.

The reason for using graphite for the nozzle and for the piece that follows the combustion port is because of it high melting point (around 3800 K), that is big enough to withstand the working temperatures of the hybrid rocket model.

Another reason for using this material is that, apart from its excellent properties it is relatively low cost.

Figure 12: First graphite mouthpiece

It is a disc with a central orifice with a smaller section than that of the propellant tube and also than the one of the post-combustion chamber placed right after it.

This contraction helps to force the appearance of turbulence at the entrance of the aforementioned chamber, which will improve the mixing of the flow gases.

Thanks to these consequences, the combustion is supposed to be completed and uniform before reaching the rocket nozzle.

The graphite mouth piece is located inside a wide metallic piece (Part 3) that serves as the propellant tubes holder.

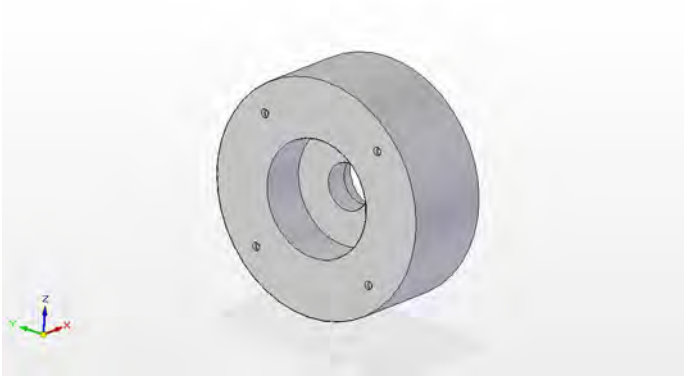

Figure 13: Stainless Piece 3

This part is the wider stainless steel item and it has two functions: one side is responsible for holding the graphite part while the other one holds the intermediate section that works as the post-combustion chamber (Part 4).

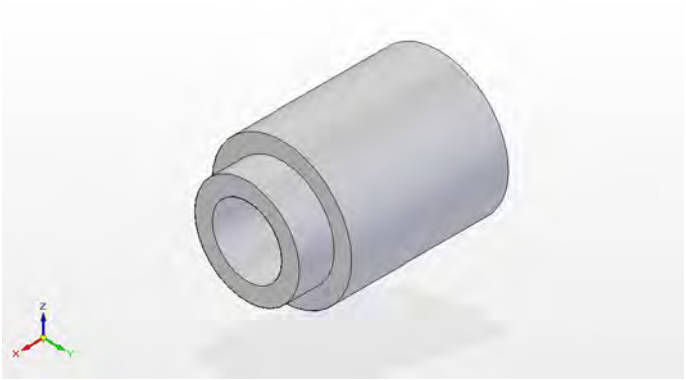

Figure 14: Stainless Piece 4

The CAD picture shown above corresponds to the above-said intermediate section. This metallic block that acts as a post-combustion chamber is a cylinder with constant section. Although it is not essential, this part has the objective of completing the combustion after the propellant port.

If we decided to remove it and place the nozzle immediately after the part 3, the fuel that has been vaporized in the final part of the port would burn in the exhaust of the rocket, causing efficiency losses and wasting some fuel.

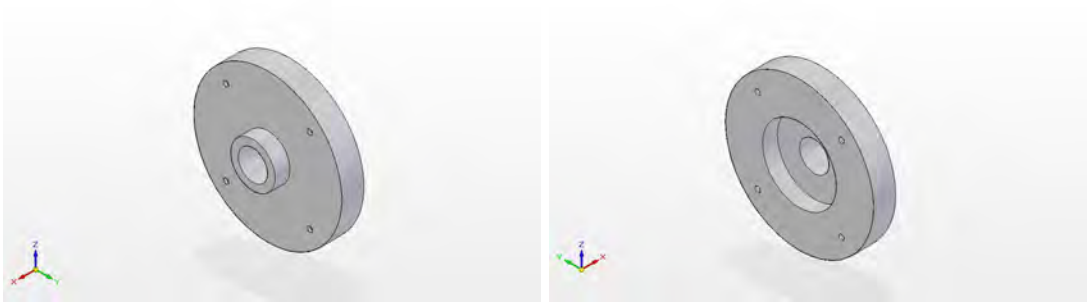

(a) Front view (b) Back view

Figure 15: Stainless Piece 5

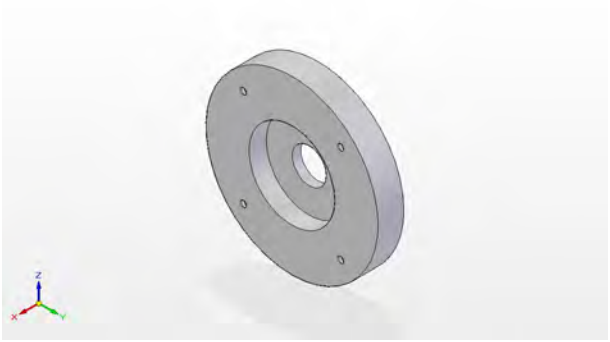

Figure 16: Stainless Piece 6

The fifth metallic piece acts as a union item between the post-combustion chamber and the graphite nozzle.
Part 5, together with part 6, have the only function of fastening the rocket nozzle. Both of them have a central orifice to allow the way of the gaseous flow to the exit of the hybrid rocket model.

Figure 17: Graphite Nozzle

The graphite nozzle is probably one of the most important parts of the nozzle.
Its function is to accelerate the fluid in the exit part to achieve the desired thrust. It has a convergent shape to ensure that the exit gases will leave in sonic conditions.

3.3 Machining of the Parts

All the parts were made from a 100 mm diameter bar of stainless steel AISI-1.4307 based on the computer aided designs made with Solid Edge. The reason to choose as the material for the rocket stainless steel is because its mechanical properties were the ones that fitted the requirements of the project. This steel, also known as inox steel, does not corrode, rust or stain when it is in contact with water or oxygen like other normal steels do. Since the rocket has to be in contact with pure oxygen, a material capable of a high resistance to corrosion was needed.
Another positive thing of this steel are its thermal properties, specifically its well conduction, specific heat and high melting point. Moreover, it is relatively easy and cheap to machine it.

The parts come from a bar with a 10 cm diameter that was cut in small pieces with an industrial hacksaw of a length 2 mm bigger than the final length of each cylinder.

Figure 18: Machining of the pieces in the lathe

The resulting piece of steel is placed in the lathe. Once the piece has been faced, a drill is made in the central part in order to make the inner diameter of the piece. Finally, it is necessary to chamfer the edges to avoid cuts when the piece is handled. This is the procedure followed to make the most part of the pieces.

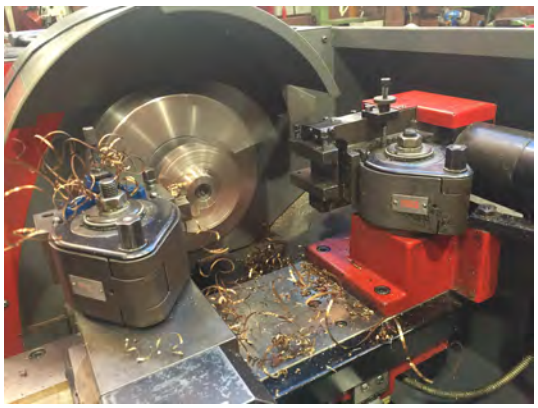

Figure 19: Machining of the pieces in the lathe

To join together all the parts of the rocket, the inox cylinders have four holes at an equidistant radius of the center by which metallic rods are passed and pieces are pressed one to another by putting wing nuts in the extremes.

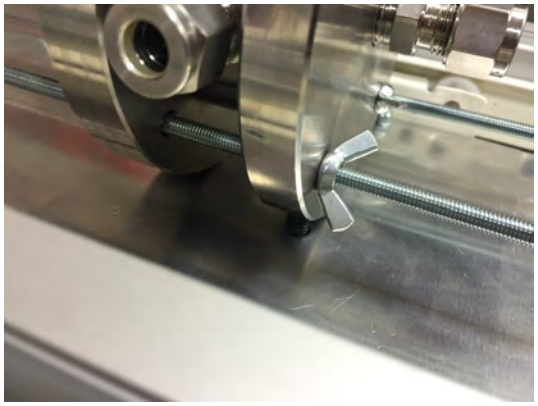

Figure 20: Wing nuts.

Also, graphite annular joints are placed at the contact points of the parts to ensure that all of them are well fixed and that there won't be gaseous leakages that could provoke an explosion in the laboratory.

3.4 Rocket assembly

All the pieces were made so that they could fit perfectly in the hole of the next part. However, to ensure that they are perfectly joined, some annular graphite pieces were placed between the parts.

In this way, we ensure that there will be no leakages when the oxygen is passing through the rocket.

The resultant assembly is shown in the following CAD pictures.

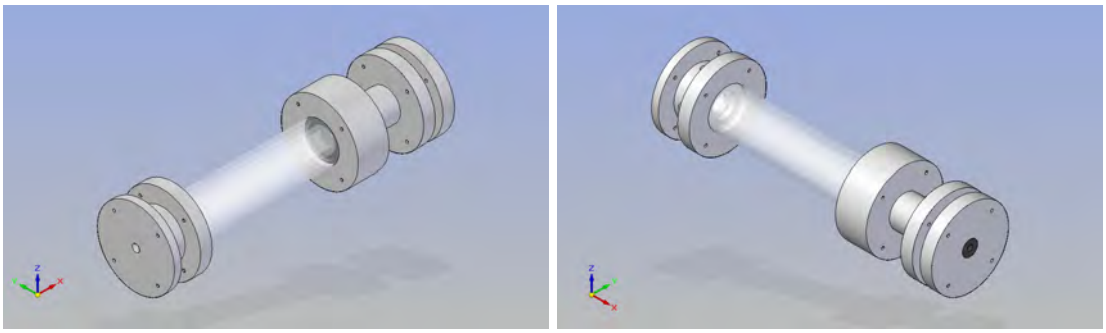

(a) Front view (b) Back view

Figure 21: Assembly of the Rocket

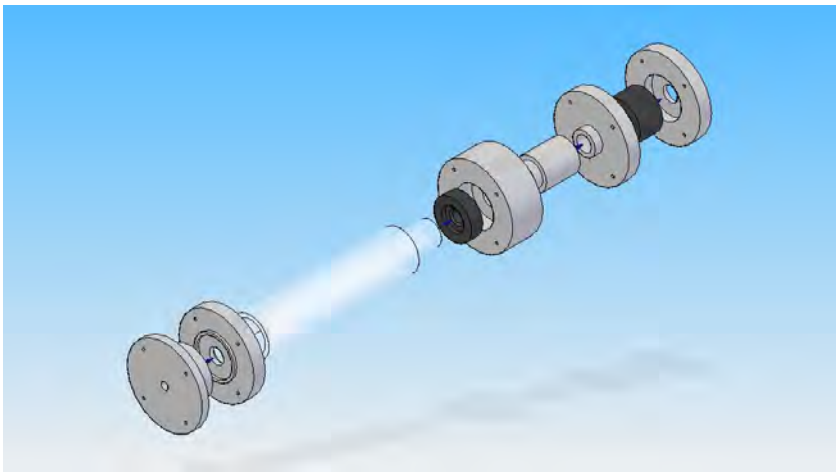

Figure 22: Assembly of the Rocket Exploded

To ensure that the system will be completely joined, some toric joints made of graphite will be placed between the different parts. They will be placed between each couple of pieces. The force necessary to seal the joint will come from tightening the screws of the rods that joint together the whole system.

Figure 23: Rods and Graphite joints

The tightening should not be too strong, since there is risk of harming the propellant block. Therefore, it is recommendable to do it manually until the assembly is solid.
Furthermore, while the firing is taking place, the pieces in contact with the voltage will expand due to the increase in temperature, but not the rods. The seal will be better then.

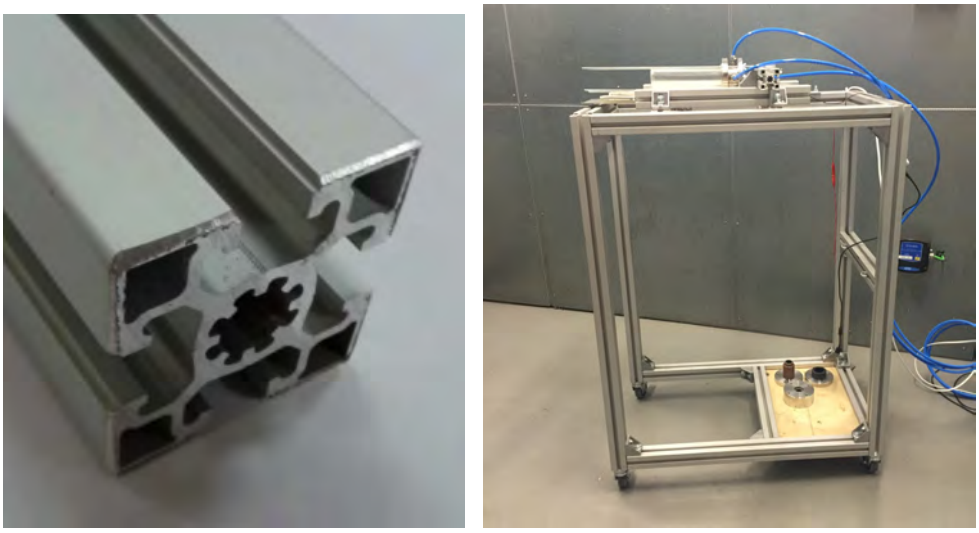

Figure 24: Aluminum profile and basic structure

The rocket is placed in a platform made of aluminum profiles. An aluminum movable plate serves as the immediate support of the rocket, that is attached to it by means of a screw placed in the upper part of the rocket.

The platform where the rocket is placed is movable to allow a small displacement so that the thrust generated by the rocket could be measured. To do the movable part it was decided to use a pair of drawer rails because of their low cost and since they could fit all the requirements: although some friction appears when the rocket is fired, it can be neglected in a first approximation, since the rocket only displaces a small distance with respect to its original position.

Using aluminum profiles for the structure permits future improvements and variations according to the new necessities.

The final result of the rocket is shown in the picture below.

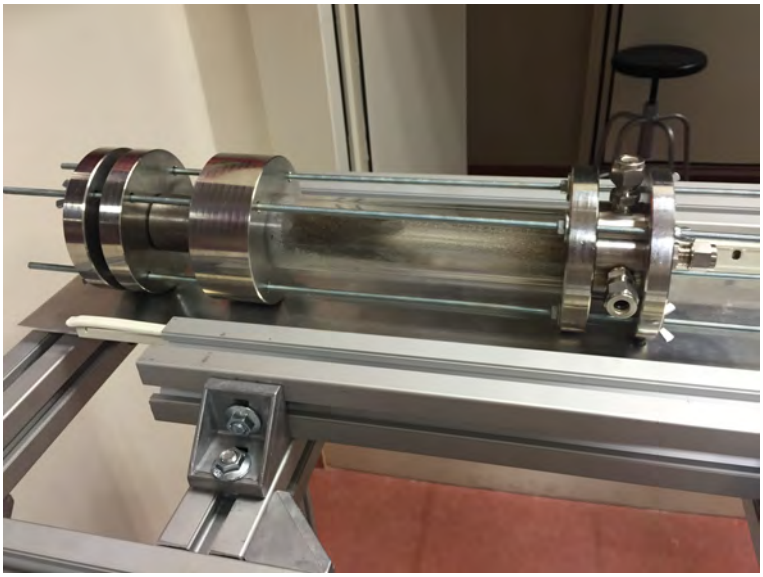

Figure 25: Final Rocket Model

3.5 Thrust measurement system

Improving the thrust measurement systems was one of the main objectives of this project, so that more accurate results could be obtained.

It was decided to use a load cell for this purpose. A load cell is a transducer whose function is to create an electrical signal directly proportional to the force that is being applied to it.

The chosen cell is the model FC22[3], which is a compression load cell. It is perfect for our project since it can measure a range of forces between 4.5 Kg and 45 kg or up to almost 450 N[4]. This cell offers normalized zero and wide range for interchangeability, as well as being able to work independently of the temperature.

Figure 26: Load Cell FC22

It is also able to measure direct force and it is not subjected to leddie fatigue failure. The load cell operates at very low strains and provides an essentially unlimited cycle life expectancy, superior resolution and a high over-range capabilities.

The cell offers normalized zero and span for interchangeability and it is thermally compensated for changes in zero and span with respect to temperature.

It is small, does not produce noise, robust, highly reliable and has a fast response time.

[3]User guide of the load cell in Annexes.
[4]User guide of the load cell in Annexes.

To measure the thrust produced by the rocket the cell is placed in the upper part of the rocket, slightly touching the external face of the part 1. The device is connected to a battery of 5 V, which is the power source, and to a voltmeter that measures the output coming from the load cell.

At the point where the cell is in contact with the rocket, the voltage given by the load cell is established as the value of zero thrust.

When the rocket is fired, the thrust will produce a small axial displacement and, in consequence, the thruster will press the load cell, giving a change in the output voltage. By applying a simple rule of three, the thrust produced by the hybrid rocket can be obtained.

In the future, it is planned to implement a new system for the data acquisition from the system. This could be done by means of programming a DAQ that immediately converts the voltage into a force, so that the thrust produced by the rocket can be obtained more easily.

4 Experimental characterization and discussion

In this section, the experiments performed with the rocket will be analyzed. First, the section will start with an explanation of the combustion reaction that takes place into the combustion port, when the PMMA is in contact with the flow of oxygen. Right after, the first firing and the way in which it was achieved is going to be analyzed and then the results obtained are going to be showed.

4.1 Combustion reaction in the propellant block

As it is already known, our model is an hybrid rocket that uses PMMA as the solid propellant while pure oxygen is used as the oxidizer. Poly(methyl methacrylate), $C_5H_8O_2$ is a widely used polymer due to its low cost and good transparency and wheatening resistance.

The PMMA, also known as poly(methyl methacrylate) comes from the acetone or propanone, organic compound with the formula $(CH_3)_2CO$, when it reacts with hydrogen cyanide, HCN, sulfuric acid, H_2SO_4, and methanol. This compound polymerizes very fast, and this process is usually done without oxygen to avoid the formation of peroxides. It is not thermally stable and it will start decomposing at 493 K approximately.[14]

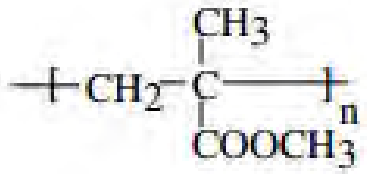

Figure 27: PMMA Monomer

The combustion process of a polymer includes the subsequent steps:

- Thermal decomposition.

- Thermal oxidative decomposition.

- Decomposition of monomer MMA.

The three steps with all the intermediate reactions in each one are explained in detail in the Annexes.

In the end, from the decomposition of the MMA monomers, small products arise. The reaction of combustion of these products can be modeled with the following reaction:

$$X + O_2 \longrightarrow CO + CO_2 + H_2O$$

Where X corresponds to methane, formaldehyde, methanol, propylene, acetone, etc.

Combustion of Small Molecules

The combustion of these small molecules leads to the creation of the ultimate products (carbon dioxide, water, carbon monoxide and some toxic gases) and to the production of heat.

- Methane combustion: It involves 26 specis and 77 elementary reactions.
- Methanol combustion: It involves 7 elementary reactions.
- Formaldehyde combustion: It involves 13 elementary reactions.
- Acetylene combustion: It is the most complex one, since it is the combination of more than 100 elementary reactions.

Kinetics of PMMA Decomposition

Polymers decomposition usually means more complex kinetics. The covalent bonds of these compounds will rotate and vibrate, creating numerous free radicals and small products that can react again between them, either creating new products or decomposing again into smaller particles.

Heat of Combustion

The heat released by the reaction is the most important parameter, since it can determine the behavior of the material when it is burned, so that thermal hazard can be estimated.

The overall reaction of incomplete burning of poly(methyl methacrylate) is:

$$-(C_5H_8O_2)-_n + aO_2 \longrightarrow bCO(g) + cCO_2(g) + dH_2O(l)$$

However, in this project it will be considered that the mixture is lean, so that all the PMMA is burned completely. This reaction can be written as:

$$-(C_5H_8O_2)-_n + 6\,nO_2 \longrightarrow 5\,nCO_2(g) + 4\,nH_2O(l)$$

According to reference [35], the heat of combustion of poly(methyl methacrylate) burning completely is 24.89 MJ/Kg.

The molecular weight of each species of the reactants and products is shown in the table below:

Species	Molecular Weight
PMMA $(C_5O_2H_8)_n$	100.1158 g/mol
Oxygen O_2	31.9988 g/mol
Carbon Dioxide CO_2	44.0095 g/mol
Water H_2O	18.0153 g/mol

Table 3: Molecular Weight of each species in the reaction of combustion of PMMA[38].

4.2 First firing and preliminary characterization

Once all the parts of the rocket have been correctly assembled by means of adjusting the bars and the wing nuts, the ports of the gases are properly joined to the holes of the first piece and the glow plug has been connected to a voltage source[5], it is possible to proceed to the ignition of the rocket.

The steps that must be followed are:

1. Open the oxygen valve until the gas flows through the tube abundantly.
2. Set the input current of the glow plug to 3 A and increase the voltage to a value around 3.2 V.
3. Open slightly the propane valve until ignition occurs.
4. Once the gas has ignited, close the propane valve and let the oxygen flow until the plume has consumed the poly(methyl methacrylate).

Since the valves or the gases can not be easily controlled, it is not possible to estimate the exact mass flow rate of oxygen and propane that should be given to the rocket to make the ignition possible. However, since the exhaust of the gases is a calibrated orifice[6], by knowing the pressure at which the gases are injected and its area, assuming that the flow exits the tube and enters the rocket with Mach number equal to 1, the mass flow rate of the gas can be known:

$$\dot{m} = \rho A_{injector} V \tag{12}$$

Where ρ can be defined with the equation of state, knowing the pressure:

$$\rho = \frac{p}{R_g T} \tag{13}$$

[5] A voltage source is a device that can produce a continuous force o move the electrons through the cables that are connected to its terminals.[39]

[6] The diameter of the orifice is 2.5mm.

And the velocity can be calculated using the equation of the Mach Number and assuming that it is equal to 1:

$$M = \frac{V}{\sqrt{\kappa R_g T}} = 1 \rightarrow V = \sqrt{\kappa R_g T} \tag{14}$$

In some of the essays, small explosions have happened when the flow of oxygen was low, possibly due to the remaining gases trapped in the pre-combustion chamber and/or at the beginning of the propellant block. In some cases, the explosion has been that big that the inner tube of PMMA has cracked.

Because of unknown reasons, it has not been possible to measure the thrust, since the voltage given by the load cell remains almost constant during the firing and equal to the calibrated value.

Due to the lack of time, it was not possible to solve this problem, and it will remain as an objective for future improvements of the project.

4.3 Test results

Despite the problems associated with the firing of the rocket and the lack of time for solving them, it was still possible to make some experiments and to take measurements from them, like the final and initial mass of the propellant tube, which gives us the mass flow rate of the gasses passing through it.

However, as it was said before, it was impossible to obtain reasonable measurements of the thrust produced by the hybrid rocket. Even after the installation of an upgraded system to measure it, some problems have appeared: for some reason, the voltage that the load cell measures while the rocket is being fired is almost the same than the one measured before the fire and that was calibrated as the zero thrust. This problems can be associated to the installation of the load cell in the structure where the rocket is placed or due to some error in the cell.
Therefore, obtaining measurements of the thrust force will continue to be an important objective for future projects concerning the rocket.

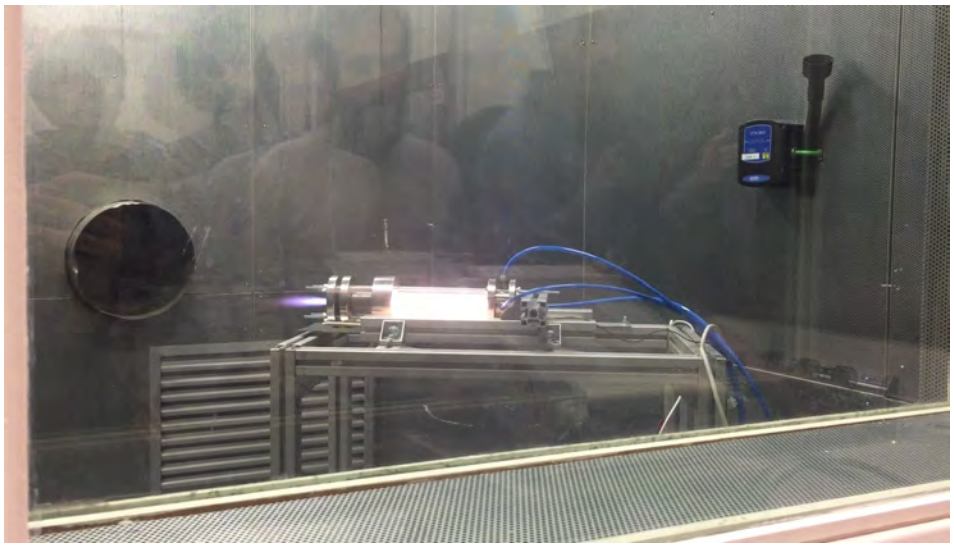

Figure 28: Firing of the rocket in the laboratory [7]

[7]The picture shows the moment in which the firing of the rocket is taking place. As it can be observed, a plume of igniting gases at high velocity exit the nozzle orifice.

Despite all that, it was possible to make some measurements of the regression rate of the rocket that, together with the measurements taken in previous experiments allow us to obtain a fitting for the mass flow rate so that parameters a and n of the following formula can be obtained:

$$r = aG^n \tag{15}$$

where r is the regression rate and G is the mass flow rate per unit area.

The first thing to do is to calculate the mass flow rate of oxygen going through the calibrated orifice. This is done with the equations of section 4.2. The experiment will be done for different pressures so that a fitting of the curve can be done to obtain the parameters a and n.

$$\dot{m_O} = \rho V A_{inj} = \frac{p}{R_g T} M \sqrt{\kappa R_g T} A_{inj} \tag{16}$$

where R_g is 287 J/KgK, T is the ambient temperature, 293.15 K, the Mach number is equal to 1, since it is considered that the gas flow is choked, and the area of the injector is equal to πR^2, with a radius of 1mm.

Experiment	Pressure	Oxygen Mass flow rate
A	4 bars	0.0052 Kg/s
B	3 bars	0.0039 Kg/s
C	2 bars	0.0026 Kg/s
D	3 bars	0.0039 Kg/s
E	2 bars	0.0026 Kg/s

Table 4: Oxygen mass flow rate

The mean fuel flow rate can be obtained by weighting the poly(methyl methacrylate) before and after the experiment and dividing the difference between the firing time:

$$\dot{m} = \frac{|\dot{m}_{final} - \dot{m}_{initial}|}{t_{firing}} \tag{17}$$

In the table below, the results of several experiments are shown:

Experiment	Initial mass	Final mass	Firing time	Mass flow rate
A	91.4 g	78.3 g	6 s	0.002183 Kg/s
B	81.2 g	55.1 g	10 s	0.002610 Kg/s
C	88.3 g	71.3 g	8 s	0.002125 Kg/s
D	92.8 g	81.8 g	7 s	0.001571 Kg/s
E	77.1 g	60.2 g	9 s	0.001878 Kg/s

Table 5: Mean flow rate

The total mass flow rate is the sum of the two previously described. Once this is known, the regression rate can be computed with the following formula:

$$\dot{m} = 2\pi R \rho_r L r \tag{18}$$

where ρ_r is the density of the material, L is the length of the tube, and r is the regression rate.

Experiment	Total Mass Flow	Regression Rate
A	0.007383 Kg/s	0.4937×10^{-3} m/s
B	0.00621 Kg/s	0.4153×10^{-3} m/s
C	0.004725 Kg/s	0.3159×10^{-3} m/s
D	0.005471 Kg/s	0.3659×10^{-3} m/s
E	0.004478 Kg/s	0.2994×10^{-3} m/s

Table 6: Total mass flow rate and Regression rate

Doing the fitting of the parameters the following values are obtained:

$a = 0.06696403$

$n = 1.000234$

5 Mathematical model

Apart from the experimental tests done with the rocket, and since there have been problems associated to them, it is interesting to develop a mathematical model that can predict the behavior of the hybrid rocket under many conditions and variables.

Therefore, in this section of the project, a mathematical one-dimensional model of the combustion process will be implemented in MATLAB in order to model analytically the firing of the rocket[8]. This model will take into account the addition of heat and mass from the walls, as well as the effects of friction that arise when the gases are flowing through the propellant tube.

However, before implementing the final model, it is necessary to explain some important concepts and the different cases that can be found when analyzing a flowing compressible gas.

5.1 Theoretical background

A fluid flow can be always modeled by using three important relations: the equation of conservation of mass, the momentum equation, and the energy equation. Additionally, the equation of state can be introduced. In the following cases it is interesting to study these equations in pairs of two depending on the situation. Hence, if we consider a flow where no frictional effects appear, only continuity and momentum equations will be studied.
Nevertheless, for the final modeling made in Matlab, the contribution of the three relations will be taken analyzed.
In this section all the effects are going to be explained and right after the general case including all the possibilities is going to be analyzed.

[8]It was expected to compare the experimental results with the ones obtained analytically but, since there have been some problems when obtaining measurements this will be no longer possible and it will be set as an objective for future improvements of the project.

5.1.1 Gas flow in a channel with changing area

To study this case, some assumptions are needed:

- The flow is one-dimensional: this assumption means that the fluid properties remain uniform in every cross-section of the channel[9].

- No frictional effects are considered: the friction forces are negligibly small and in a first approximation the fluid is considered as isentropic.

- There is no heat exchange between the fluid and the surroundings and neither is work.

For this case, the equation of continuity is to be analyzed:

$$\frac{d\rho}{\rho} + \frac{dA}{A} + \frac{dV}{V} = 0 \tag{19}$$

From this equation it can be predicted that at Mach number equal to unity the area goes through a minimum for any kind of fluid (liquid or gaseous).

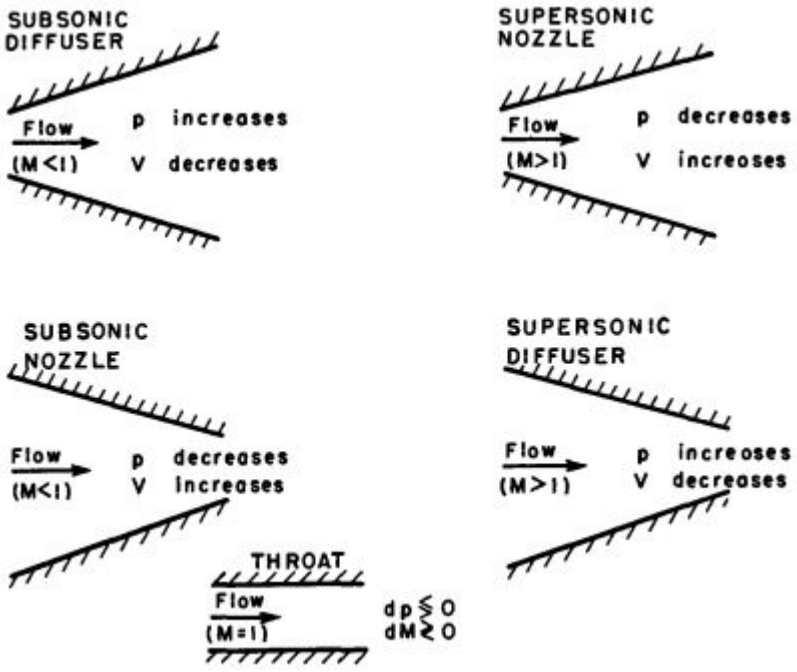

Figure 29: Effects of the change of area in the Mach number, pressure and temperature.

[9]The approximation of a one-dimensional fluid provides a high simplicity and rapid and easy calculation methods. Furthermore, the results obtained are reliable and very useful.

5.1.2 Gas flow in constant area channels with friction

To study the behavior of a gas stream flowing through a duct with constant area under the effects of friction, the following assumptions will be made:

- The flow is one-dimensional.

- There is no heat exchange between the fluid and the surroundings and neither is work.

- The flow is steady.

- The cross-sectional area is constant.

- The effects due to elevation will be neglected.

In this case, the equations of continuity and energy can be written as:

$$\frac{w}{A} = \rho V \equiv G \tag{20}$$

$$h + \frac{V^2}{2} = h_0 \tag{21}$$

where, G is the mass velocity, V is the flow velocity, and h and h_0 are the enthalpy and stagnation enthalpy respectively.

Combining both equations it is possible to obtain the equation of the *Fanno Line*:

$$h = h_0 - \frac{G^2}{2\rho^2} \tag{22}$$

These lines can be represented in a $h - v$ or a $h - s$ diagram, as it is shown below:

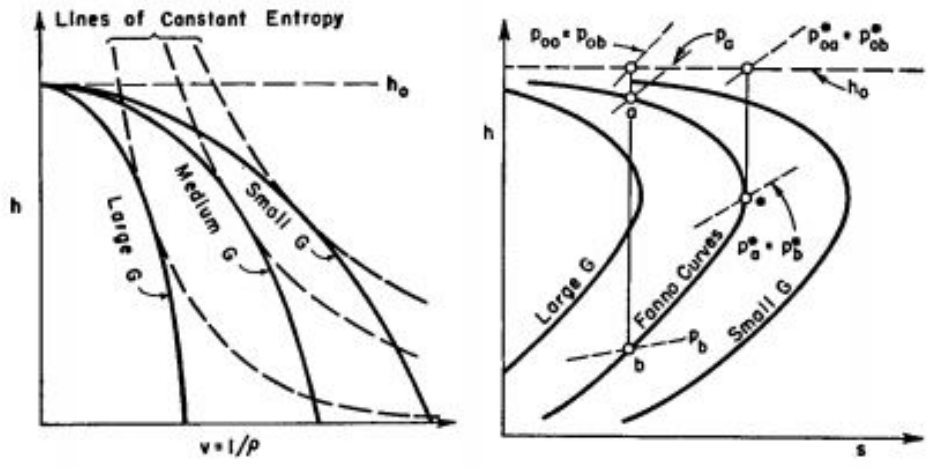

Figure 30: Fanno Line

Analyzing them it can be observed that, due to the effects of friction, the flow will always tend to reach sonic conditions both in the subsonic and supersonic branches, even if the area does not change. Therefore, if the flow is subsonic at some point, the effects of friction will be to increase its velocity and to decrease the pressure and enthalpy. On the other hand, if the flow is supersonic, friction will produce a decrease in Mach Number and an increase in pressure and enthalpy.

A summary of the frictional effects in a gas-stream flowing through a pipe of constant area is:

	Subsonic	Supersonic
Pressure p	decreases	increases
Temperature T	decreases	increases
Velocity V	increases	decreases
Density ρ	decreases	increases
Mach Number M	increases	decreases
Stagnation Pressure p_0	decreases	decreases
Impulse function, F	decreases	decreases

Table 7: Frictional Effects in a 1D Flow [8]

The Mach number always tends to reach unity. Hence, the flow will be choked most of the times due to frictional effects.

5.1.3 Flow in a channel with heat addition

When heat is added to a flow, the process that takes place is that comprising variations in stagnation temperature and stagnation enthalpy. It will be assumed that this changes occur in an ideal gas stream flowing through a duct with constant cross-sectional area and with no friction.

In the reality these conditions are difficult to achieve since a change in stagnation temperature by means of an external source of heat ensure that friction will appear due to the dependence between the friction mechanisms and heat transfer. In a similar way, the

chemical composition and the mass rate of the gas stream will change if the stagnation temperature is increased or decreased.

This simplified modelling is known as the process of *Simple T_0-Change*.

In this case, the equations of continuity and the momentum equation can be written as:

$$\rho V = \frac{w}{A} = G = \text{constant} \tag{23}$$

$$p - \rho V^2 = \frac{F}{A} \tag{24}$$

Combining both equations, the *Rayleigh Line* relation is obtained:

$$p + \frac{G^2}{\rho} = \frac{F}{A} \tag{25}$$

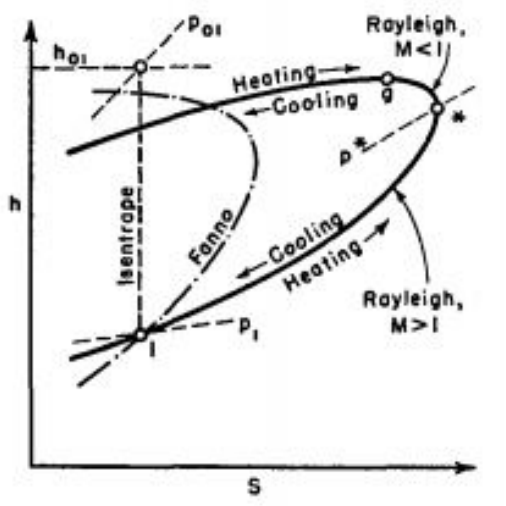

As it can be observed in the graph, the part of the line above the point where the entropy is maximum corresponds to subsonic flow while the other part corresponds to the supersonic flow.

Since the process of simple heating that is being taken into account is thermodynamically reversible, the addition of heat produces an increase of entropy and heat extraction corresponds to a decrease of entropy.

Therefore, at supersonic speeds (lower branch), Mach Number is decreased by the addition of heat, while cooling increases the Mach Number. In subsonic flow (upper branch), the effect is the opposite: Mach Number will increase when the flow is heated and it will

decrease if the flow is cooled.
In other words, heating the fluid always produces a change towards the point where the Mach Number is unity. This effect always causes a reduction in the stagnation pressure and an increase in the stream temperature.

The effects of changes in the stagnation temperature T_0 are shown in the table below:

	Heating M < 1	Heating M > 1	Cooling M < 1	Cooling M > 1
Pressure, p	decreases	increases	increases	decreases
Temperature, T	Note (1)	increases	Note (2)	decreases
Velocity V	increases	decreases	decreases	increases
Mach Number M	increases	decreases	decreases	increases
Stagnation Pressure p_0	decreases	decreases	increases	increases
Stagnation Temperature, T_0	increases	increases	decreases	decreases
Note (1): increases for M $< 1/\sqrt{k}$, and decreases for M $> 1/\sqrt{k}$				
Note (2): decreases for M $< 1/\sqrt{k}$, and increases for M $> 1/\sqrt{k}$				

Table 8: Heating and Cooling Effects in a 1D Flow [8]

Choking Effects in Simple T_0-Change

- Increase in Stagnation Pressure: If the stagnation pressure is increased, there is a maximum stagnation temperatures ratio is possible for each initial Mach Number. Also, for a fixed initial stagnation temperature, there is a maximum permitted initial Mach Number.

- Decrease in Stagnation Temperature: When the fluid is cooled, it does not exist a limit in the stagnation temperature ratio, since the initial Mach Number is lower than unity. Nevertheless, for initial supersonic flows, there is a maximum allowed reduction in stagnation-temperature ratio for any initial Mach Number. [8]

5.1.4 Generalized one-dimensional flow

Now, the case in which all the effects previously stated occur simultaneously will be analyzed.

The effects taken into account are:

- Change in area.
- Frictional effects.
- Heat exchange with the surroundings.
- Change in the chemical composition.
- Changes in molecular weight, chemical reaction and change of phase.

Also, some hypotheses are needed:

- The flow is steady and one-dimensional.
- The changes in the flow properties are continuous.
- The gas used is almost perfect.

Taking into account all that has been previously stated, we end up with the following equations [8]:

Equation of State:

$$\frac{dp}{p} = \frac{d\rho}{\rho} + \frac{dT}{T} - \frac{dW}{W} \tag{26}$$

Mach Number:

$$\frac{dM^2}{M^2} = \frac{dV^2}{V^2} + \frac{dW}{W} - \frac{d\kappa}{\kappa} - \frac{dT}{T} \tag{27}$$

Continuity Equation:

$$\frac{dw}{w} = \frac{d\rho}{\rho} + \frac{dA}{A} + \frac{dV}{V} \tag{28}$$

Energy Equation:

$$\frac{dQ - dW_x + dH}{c_p T} = \frac{dT}{T} + \frac{\kappa - 1}{2} M^2 \frac{dV^2}{V^2} \tag{29}$$

Momentum Equation:

$$\frac{dp}{p} + \frac{\kappa M^2}{2}\frac{dV^2}{V} + \frac{\kappa M^2}{2}\left(4f\frac{dx}{D} + \frac{dX}{\frac{I}{2}\kappa pAM^2}\right) + \kappa M^2(1-y)\frac{dw}{w} = 0 \tag{30}$$

If all these equations are combined a solved as a system of differential equations, the entire flow pattern can be modeled, and the behavior of the gas-stream can be known at any point.

Analyzing the effects of increasing independent parameters in the Mach Number and Stagnation Pressure it is obtained that:

	Subsonic (M < 1)	Supersonic (M > 1)
Area Increased	decreases	increases
Heating	increases	decreases
Effect of Friction	increases	decreases
Mass Flow Increased	increases	decreases
Molecular Weight Increased	decreases	decreases
k Increased	decreases	decreases

Table 9: Effect of Independent Parameters in Mach Number[8]

	Stagnation Pressure, p_0
Change in Area	-
Stagnation Temperature Increased	decreases
Effect of Friction	decreases
Gas injection ($y < 1$)	decreases
Molecular Weight Increased	decreases
k Increased	decreases

Table 10: Effect of Independent Parameters in Stagnation Pressure [8]

5.2 Assumptions and hypotheses for the hybrid rocket model

- One-dimensional model: all the fluid properties remain uniform in every cross-section of the duct.
- It is assumed that the changes in the flow properties are continuous, which means that the variation is the same in each differential of the position.
- It will be considered that there is change of area, heat addition and mass addition.
- The specific heats at constant volume, c_v and at constant pressure, c_p, and therefore the adiabatic gas constant κ and R change in a prescribed way.

5.3 Model equations

Since for our particular model all the possibilities are being considered, all the equations for mass conservation, momentum equation and energy equation have to be integrated together, opposite to the previous models described in section 4.1, where one of these equations could be neglected.

Therefore, we end-up with the following relations:

Continuity Equation:

$$\frac{dw}{w} = \frac{d\rho}{\rho} + \frac{dA}{A} + \frac{dV}{V} \tag{31}$$

Momentum Equation:

$$\frac{dp}{p} + \frac{\kappa M^2}{2}\frac{d(V^2)}{V^2} = -2\kappa M^2 f\frac{dx}{D} + \Big(\frac{V_{in}}{V} - 1\Big)\kappa M^2\frac{dw}{w} \tag{32}$$

Energy Equation:

$$w\Big(c_p dT + d\frac{V^2}{2}\Big) = \Big(h_{in} - h + \frac{V_{in}^2 - V^2}{2}\Big)dw + w dh_{reac} + d\dot{Q} \tag{33}$$

The previous three equation are written taking logarithmic differentials to facilitate the integration.

They have to be solved in order to obtain the variation of the temperature, T, the pressure, p, the density, ρ and the velocity, V, over the distance x.

Since there are three equations for four unknowns, another equation is needed: the equation of state:

$$p = \rho RT \tag{34}$$

that, written in logarithmic form is:

$$\frac{dp}{p} = \frac{d\rho}{\rho} + \frac{dT}{T} - \frac{dW}{W} \tag{35}$$

The four equations have to be implemented in a Matlab code, and they are solved using the function *ode*45.

However, Matlab need the equations to be solved for the differential of the four unknown. In consequence, they must be combined so that we end-up with a system of four equations for $dV, dT, d\rho$ and dp.

This system is obtained by dividing all the formulas by dx and solving the continuity, momentum and energy equations for $d\rho$, dp and dT respectively and introducing them in the equation of state:

$$\frac{dw}{w} = \frac{d\rho}{\rho} + \frac{dA}{A} + \frac{dV}{V} \Longrightarrow d\rho = \rho\Big[\frac{dw}{w} - \frac{dA}{A} - \frac{dV}{V}\Big] \tag{36}$$

$$\begin{aligned} \frac{dp}{p} + \frac{\kappa M^2}{2}\frac{d(V^2)}{V^2} = -2\kappa M^2 f\frac{dx}{D} + \Big(\frac{V_{in}}{V} - 1\Big)\kappa M^2\frac{dw}{w} \Longrightarrow \\ dp = p\Big[\Big(\frac{V_{in}}{V} - 1\Big)\kappa M^2\frac{dw}{w} - \frac{2\kappa M^2 f}{D} - \frac{\kappa M^2}{V}dV\Big] \end{aligned} \tag{37}$$

$$\begin{aligned} w\Big(c_p dT + d\frac{V^2}{2}\Big) = \Big(h_{in} - h + \frac{V_{in}^2 - V^2}{2}\Big)dw + wdh_{reac} + d\dot{Q} \Longrightarrow \\ dT = \Big(\frac{\Big[\Big(h_{in} - h + \frac{V_{in}^2 - V^2}{2}\Big)dw + wdh_{reac} + d\dot{Q}\Big]}{wc_p}\Big) - \frac{VdV}{c_p} \end{aligned} \tag{38}$$

$$\frac{dp}{p} = \frac{d\rho}{\rho} + \frac{dT}{T} - \frac{dW}{W} \Longrightarrow \Big(\frac{V_{in}}{V} - 1\Big)\kappa M^2 \frac{dw}{w} - \frac{2\kappa M^2 f}{D} - \frac{\kappa M^2}{V} dV = \frac{dw}{w} - \frac{dA}{A} - \frac{dV}{V} + \frac{\Big[\Big(h_{in} - h + \frac{V_{in}^2 - V^2}{2}\Big)dw + w dh_{reac} + d\dot{Q}\Big]}{w c_p T} - \frac{V dV}{c_p T} - \frac{dW}{W} \tag{39}$$

Finally, the resulting system of equations is:

$$dV = \frac{\Big(\frac{V_{in}}{V} - 1\Big)\kappa M^2 \frac{dw}{w} - \frac{2\kappa M^2 f}{D} - \frac{dw}{w} + \frac{dA}{A} - \frac{\Big[\Big(h_{in} - h + \frac{V_{in}^2 - V^2}{2}\Big)dw + w dh_{reac} + d\dot{Q}\Big]}{w c_p T} + \frac{dW}{W}}{\kappa M^2 - \frac{1}{V} - \frac{V}{c_p T}} \tag{40}$$

$$d\rho = \rho\Big[\frac{dw}{w} - \frac{dA}{A} - \frac{dV}{V}\Big] \tag{41}$$

$$dp = p\Big[\Big(\frac{V_{in}}{V} - 1\Big)\kappa M^2 \frac{dw}{w} - \frac{2\kappa M^2 f}{D} - \frac{\kappa M^2}{V} dV\Big] \tag{42}$$

$$dT = \Big(\frac{\Big[\Big(h_{in} - h + \frac{V_{in}^2 - V^2}{2}\Big)dw + w dh_{reac} + d\dot{Q}\Big]}{w c_p}\Big) - \frac{V dV}{c_p} \tag{43}$$

To obtain the solution from the integration of this equation, there are many variables that have to be determined, either by giving them a fixed value or by stating them as a function of the position of the flow:

- The terms V_{in} describes the velocity with with the mass flow is injected from the walls to the fluid. In a first approximation this term is going to be considered equal to zero.

- The change of enthalpy will be constant along the duct, making the term $h_{in} - h = 0$ at any point of the duct. This is because we assume that the wall is at the same temperature that the flow going through the central axis. Since the enthalpy can be described as:

$$h = c_p \Delta T \tag{44}$$

if the change in temperature is zero, so is the change in enthalpy.

- The gas properties, such as κ, c_p, c_v and R will be obtained as a function of the position, and the following hypothesis will be made: It will be considered that the gas properties upstream are those corresponding to the properties of pure oxygen, while downstream, the exhaust gases will be a mixture between carbon dioxide and water. Also, it will be assumed that the variation along the duct is linear. Therefore, the gas properties change in the following way:

Gas	κ	c_p [J/molK]	c_v [J/molK]	R [J/molK]
O_2(g) @ 298 K	1.4	29.4	21	8.4
CO_2(g) @ 4000 K	1.16	63.23	54.28	8.95
H_2O(g) @ 4000 K	1.33	57.9	43.53	14.37

Data obtained from references [27, 29, 30]

Table 11: Properties of the combustion gases.

The specific heat at constant volume and the gas constant R are computed from the following equations, while the values of c_p and κ are obtained from the literature:

$$\kappa = \frac{c_p}{c_v} \tag{45}$$

$$R = c_p - c_v \tag{46}$$

Finally, the relation obtained for the gas properties as a function of the position x is the following:

- Initial composition: O_2
- Final composition: 5 moles of CO_2 per 4 moles of H_2O

The graphical distribution of the flow properties can be described as:

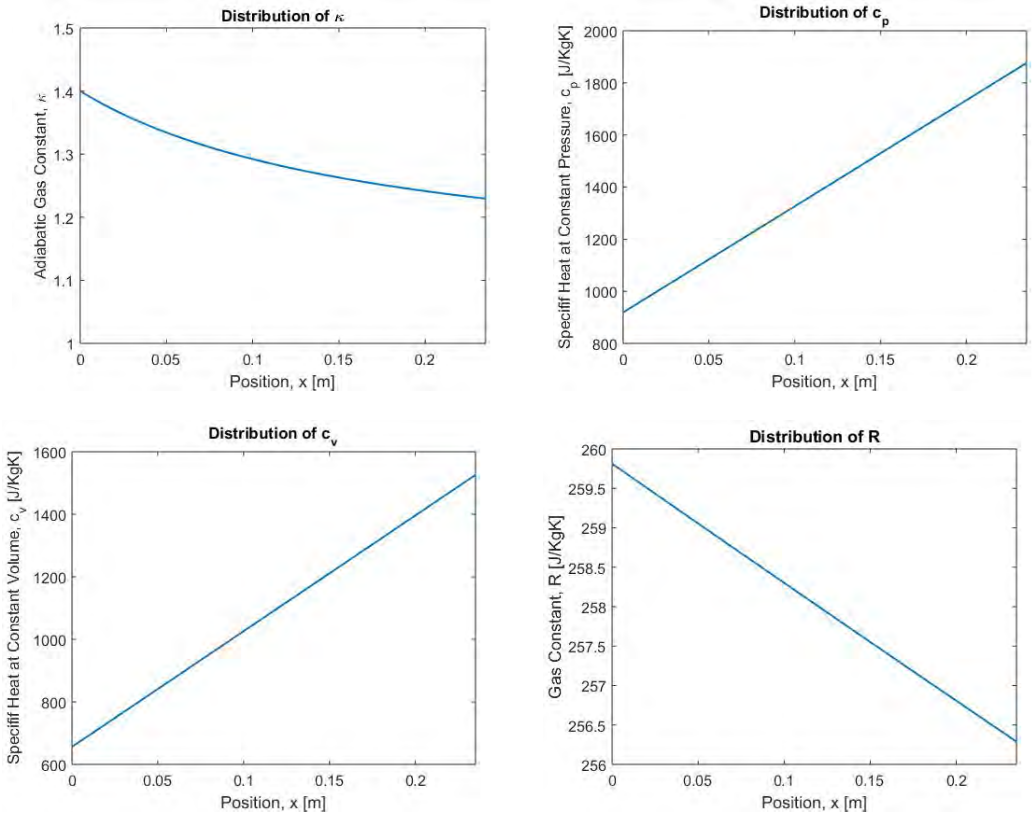

Figure 31: Distribution of κ, c_p, c_v and R along the combustion duct

- To make the integration easier, the Mach number will be written as a function of the velocity at that point.

- The mass flow rate w is written also as a function of the position and it is determined with equation (20).

- The mass flow differential is characterized with the following relation:

$$dw = \frac{aG^n}{A_{lateral}} \tag{47}$$

where G is the mass flow per unit area, and a and n are constants obtained experimentally. The reason to use this expression is because it corresponds to the model for the fuel mass flow in a hybrid rocket channel. [31, 32, 33]

To simplify the model it will be assumed that G is equal to the product of the initial density times the initial velocity:

$$G = \rho_0 V_0 \tag{48}$$

The value of the constants a and n was calculated in section 4.2 by fitting the curve from the experimental results obtained for the regression rate and the mass flow rate.

Therefore, it is assumed that the parameters a and n have the following values:

a= 6.69×10^{-2}

n=1.000234

- The friction factor is estimated from the literature. It was found that for smooth PMMA it is equal to 0.54. However, since as the combustion takes place, the poly(methyl methacrylate) undergoes erosion, and the surface is seen to be not smooth, the friction factor will be multiplied by a reasonable factor of 3.

- The term dh_{reac} corresponds to the change in enthalpy due to the combustion of the PMMA multiplied by the differential of mass flow rate. This value is obtained from the literature and it is equal to $24.89 MJ/Kg$ [10].

- In the first and last equations it can be seen that the term $d\dot{Q}$ appears. This corresponds to the addition and rejection of heat from the walls. It is computed per differential of the position x and it is a function of the differential of the mass flow rate per unit area and a constant:

$$d\dot{Q} = Cdw = -(\Delta H_{sub} + \Delta T c_p)dw \tag{49}$$

  The constant C, in turn, is a function of the specific heat capacity at constant pressure of PMMA, its enthalpy of sublimation and of the change in temperature to which it is subjected:

ΔH_{sub}	600.7 kJ/Kg
c_p	1500.2 J/KgK

Data obtained from references [14]

Table 12: Properties of PMMA

- The terms W and dW correspond to the molecular weight of the flowing gases and to its derivative with respect to the axial position in the duct.

  From the relation of the ideal gases, the molecular weight can be written as:

$$W = \frac{\rho R T}{p} \tag{50}$$

As it was previously stated, the four parameters change as the flow moves forward, so it has to be defined at every point, and the same for its derivative dW.

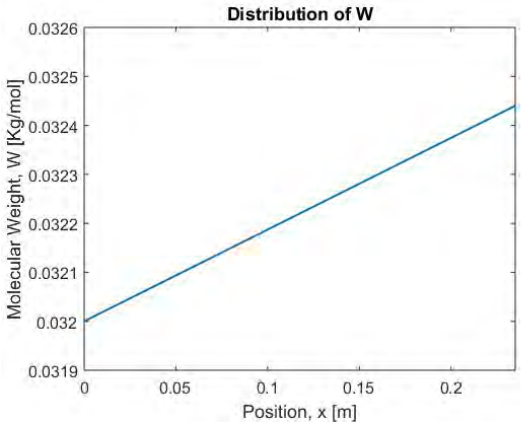

Figure 32: Model of the distribution of the molecular weight along the duct

- The last term needed to described is the area by which the flow passes and its derivative. For the one-dimensional model, two main sections are considered: first a long duct with constant radius (which corresponds to the PMMA tubes) and then a convergent nozzle by which the exhaust gases exit the port.

  The shape given to it is the following:

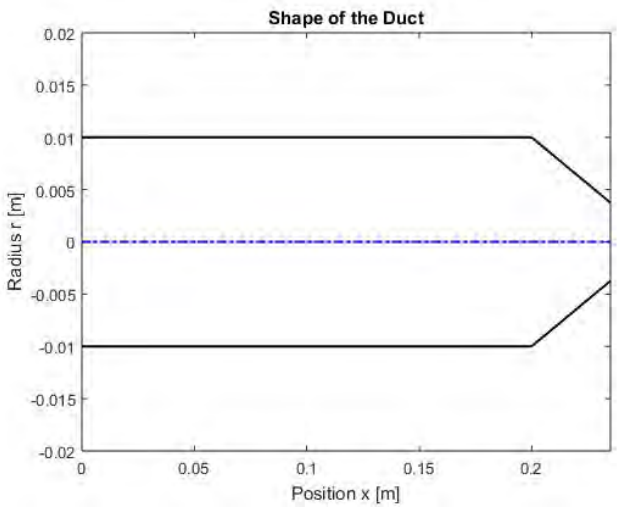

Figure 33: Radius distribution of the duct for the mathematical one-dimensional model

5.4 Matlab code

The Matlab Code created to solve the one-dimensional model has the following structure: It is composed of several functions:

- One including the equations that need to be integrated and that gives as an output the derivative of the four properties, V, ρ, p, T.
- Another function that gives the flow properties (the distribution of κ, the specific heat at constant pressure and at constant volume, R and the molecular weight.
- A third function gives as an output the differential of mass flow rate.
- There is another function that provides the distribution of heat and enthalpy.
- The last function is the one that states the distribution of the area and its differential along the duct.

The problem is solved in the following way: the first function obtains the results from the rest of functions and uses these outputs as inputs to solve the equations.

This main function is solved using *ode*45, which integrates the function over all the length of the duct, which includes the PMMA tube and the nozzle, giving the final distribution of the four variables: velocity, density, pressure and temperature.

However, the process is more complex since the solution does not converge when the Mach number reaches unity, creating instabilities. For this reason it was decided to make a three-steps integration method:

First, the equations are integrated until the Mach number is close to unity, for example 0.95. When this happens, the integration stops and some integration steps are done "by hand", considering that the derivatives of the variables remain constant in this interval. This step is done until the Mach number is somewhere above unity, for example 1.05. When this happens, the equations are integrated again with *ode*45 until the end of the duct.

The variables that consider the addition of heat, mass and the effects of friction acting on the flow are only considered in the tube of PMMA. The nozzle only considers the effects due to the change in area.

Apart from this, since the code must look after the configuration for which the Mach Number is equal to unity at the exit section, the results are iterated until the initial conditions that fulfill this requirement are found.

5.5 Hybrid rocket simulation and performance prediction

In this section, the results obtained from the Matlab Code are going to be explained. Several cases have been studied:

1. The case in which only the change in area is taken into account, at both ambient temperature 298 K and when the flow enters with higher temperature.
2. The case in which the friction effects are considered together with the change in area, at 298 K.
3. The case in which the mass flow rate coming from the walls is considered together with the change in area, at 298 K.
4. The general case in which all the effects are considered: heat and mass addition from the walls, friction forces and change in area, at 298 K.

The results are going to be discussed and compared between them in order to obtain a reasonable conclusion concerning the behavior of the flow under several conditions.

5.5.1 Change in Area

As it has been already seen in the theoretical background, this is the simplest effect to which a flow can be subjected. It only considers the variation of the radius of the duct, neglecting any other effect such as heat or mass addition. The objective was to analyze the flow in order to obtain sonic conditions in the nozzle exhaust.

As it was explained in section 4.3, the mass flow rate entering the rocket can be calculated, since it is going through a calibrated orifice of 2mm diameter and it is assumed that the Mach number in the hole is equal to one. The total pressure is the same after the hole, 298 K, but the total pressure is not conserved.

Knowing that the mass flow is conserved from one point to another, it can be stated that the product ρV is constant. However, it is necessary to iterate to find the initial conditions of the flow at the entrance of the tube that give sonic conditions at the exit of the nozzle.

In this case, where only the change in area is being considered, the initial conditions are the following: the flow enters the rocket with a temperature of $298K$, a density of $1.331Kg/m^3$[10] and a pressure of $3bar$. Therefore, $V = 24.65m/s$.

As it can be observed in the plots below, all the properties remain constant along the propellant block and when they reach the nozzle the variation is exponential. The velocity increases while the density, pressure and temperature decrease during the contraction of the tube.

The fifth plot shows that the Mach number remains low along the propellant tube and then it increases until reaching unity at the exit of the nozzle.
These conditions (M = 1) where found for an initial velocity of 24.65 m/s when the initial temperature is equal to the ambient temperature, as it was previously stated.

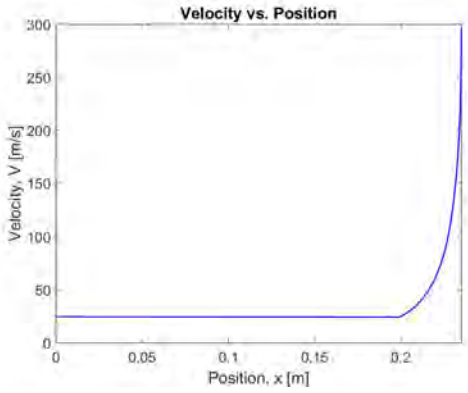

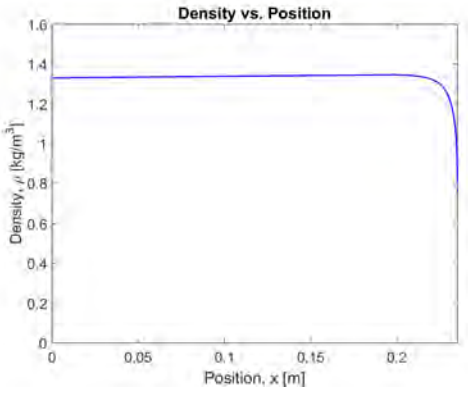

[10]Density of pure oxygen at ambient temperature. [30]

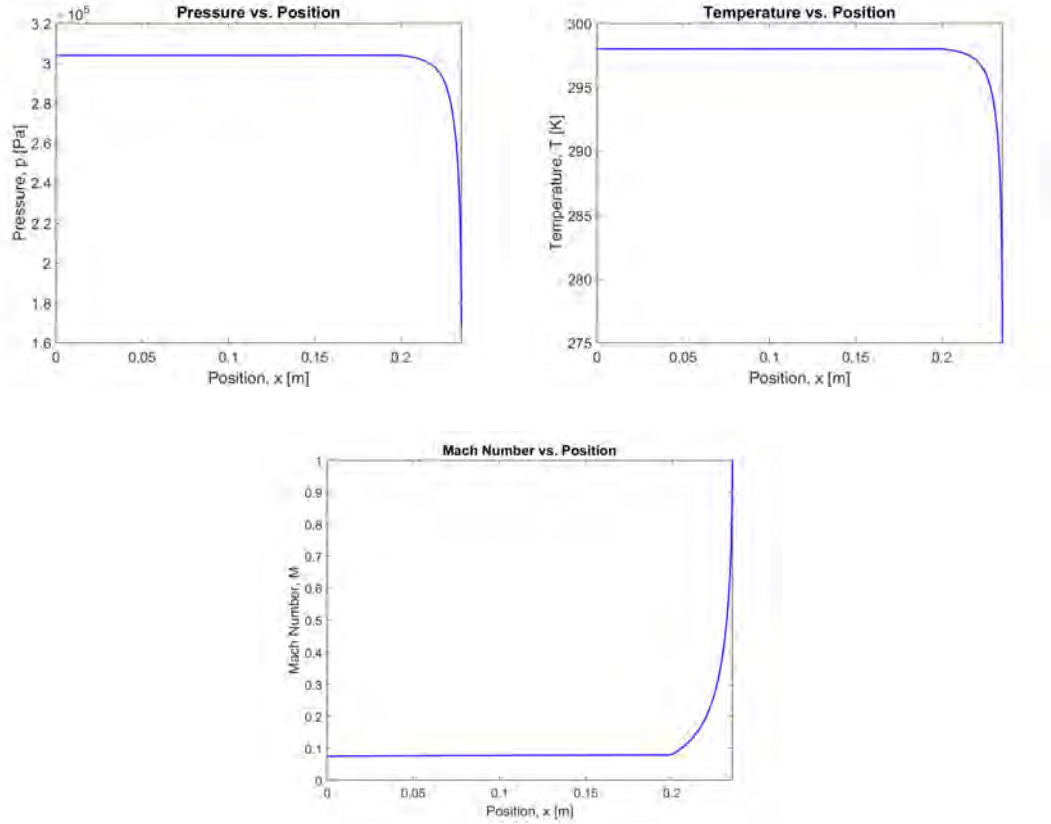

Figure 34: Distribution of the variables V, ρ, p, T and Mach Number over the position considering only the change in Area when the flow enters at 298 K.

If now the flow is introduced at a higher temperature, for example 500 K, the effects are the following:

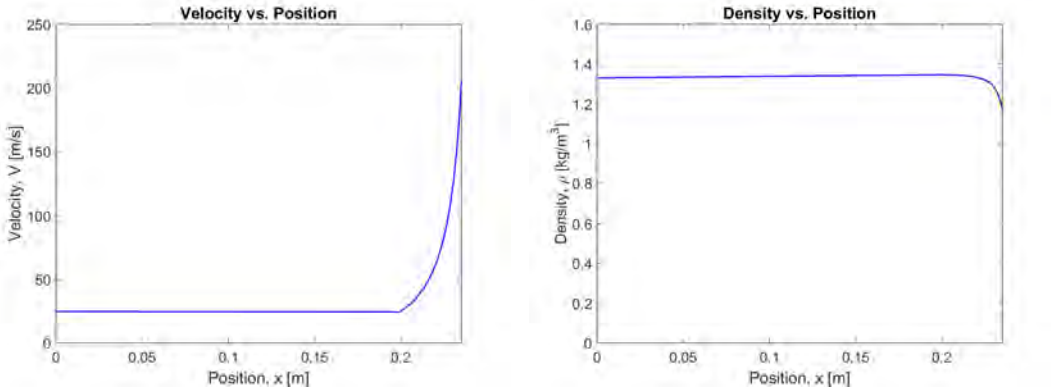

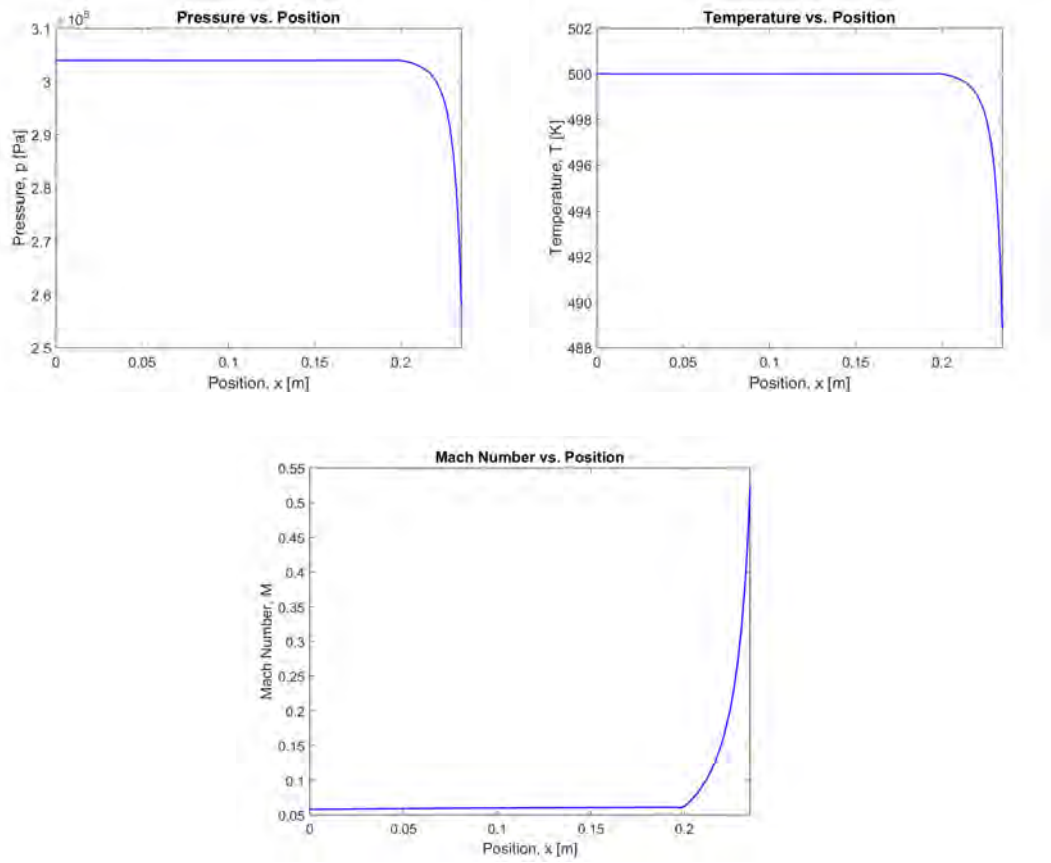

Figure 35: Distribution of the variables V, ρ, p, T and Mach Number over the position considering only the change in Area when the flow enters at 500 K.

It can be observed that the behavior of the variables is almost the same. However, it can be noticed that the Mach number at the exit is now reduced more or less to the half, 0.52.

From this results, it can be stated that increasing the temperature of the flow at the entrance is going to decrease its velocity and as a consequence the flow will be subsonic all along the duct, moving the sonic region downstream. Although in our experiment there is little or no control over the temperature at the entrance, it is interesting to analyze the effect that raising the temperature would have in the flow.

5.5.2 Change in Area and Frictional Effects

In this section the friction effects are going to be added to the previous case in which only the change in area was considered. The results for the same entrance velocity and ambient temperature at the inlet showing that the iterative procedure is necessary are shown below:

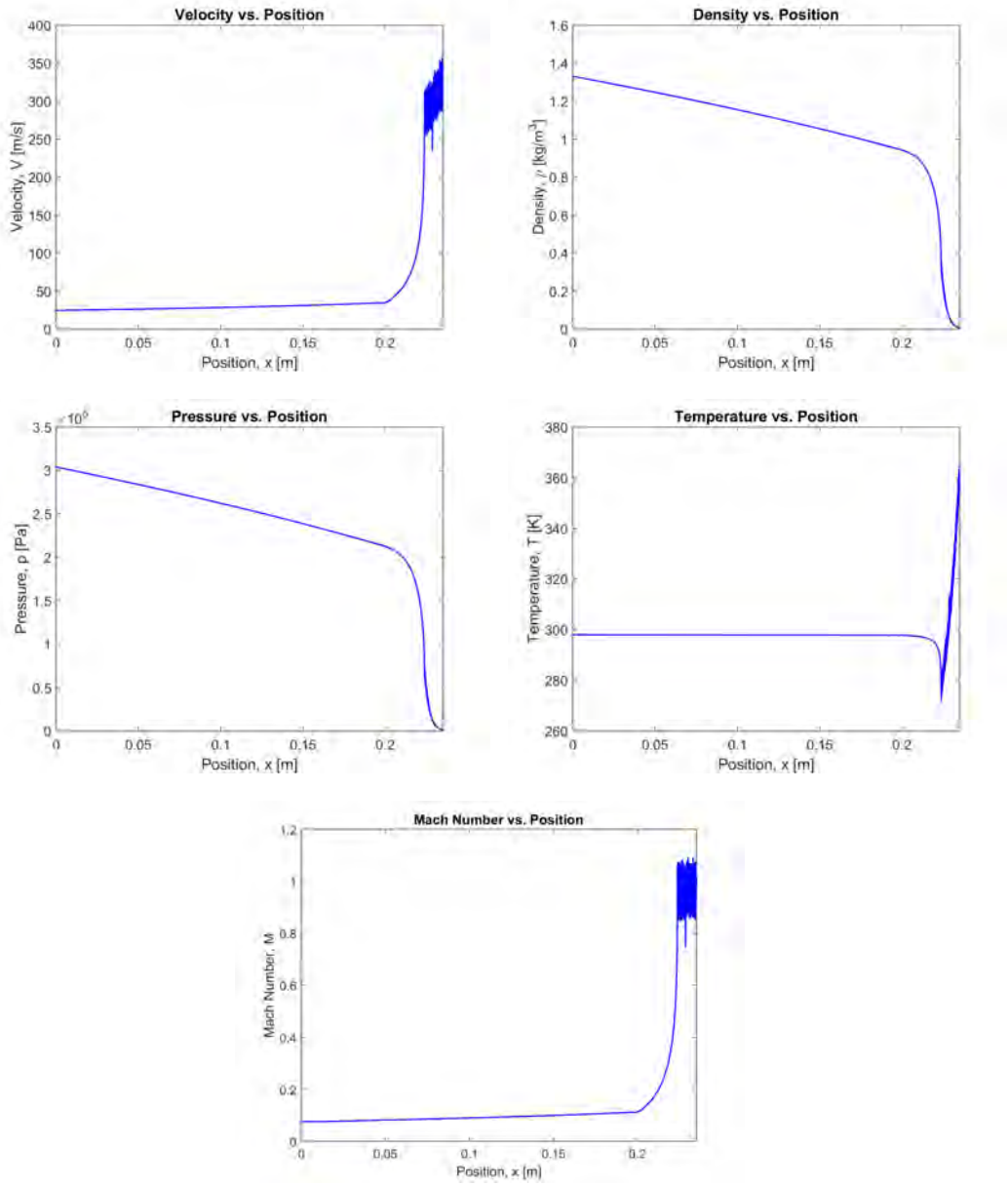

Figure 36: Distribution of the variables V, ρ, p, T and Mach Number over the position considering the change in Area and the frictional effects when the flow enters at 298 K and 24.65 m/s, showing that the iterative procedure is necessary.

As it can be observed, introducing this effect creates an instability in the behavior of the properties. As the theory predicted, the friction forces move the sonic section upstream, provoking a shock in the middle of the nozzle that Matlab traduces as a non-convergence.

Besides, it can be appreciated that now the properties are not constant along the propellant tube, and they increase or decrease linearly.

Since the objective is to find the initial conditions with which the flow will reach mach number equal to unity at the exit section, a manual iterative procedure is followed:
The initial velocity of the flow is lowered until the sonic region is displaced to the outlet section. However, since the continuity equation must be constant at any time, the density must be varied according to the change of velocity to keep the mass flow constant:

$$\dot{m} = \rho A V \tag{51}$$

Since the Area is the same for all the cases, it can be written that:

$$\rho V = constant \tag{52}$$

Apart from changing the density, it is also necessary to adjust the rest of properties of the flow. To calculate the pressure, the static temperature is computed at the entrance with the following formula:

$$T_t = T\Big(1 + \frac{\kappa - 1}{2} M^2\Big) \tag{53}$$

Once the temperature is known, the injection pressure can be computed with the equation of state:

$$p = \rho R T \tag{54}$$

Therefore, for this case it was found that the necessary inlet conditions were:

$$V = 12.885 m/s$$
$$p = 2.613 bar$$

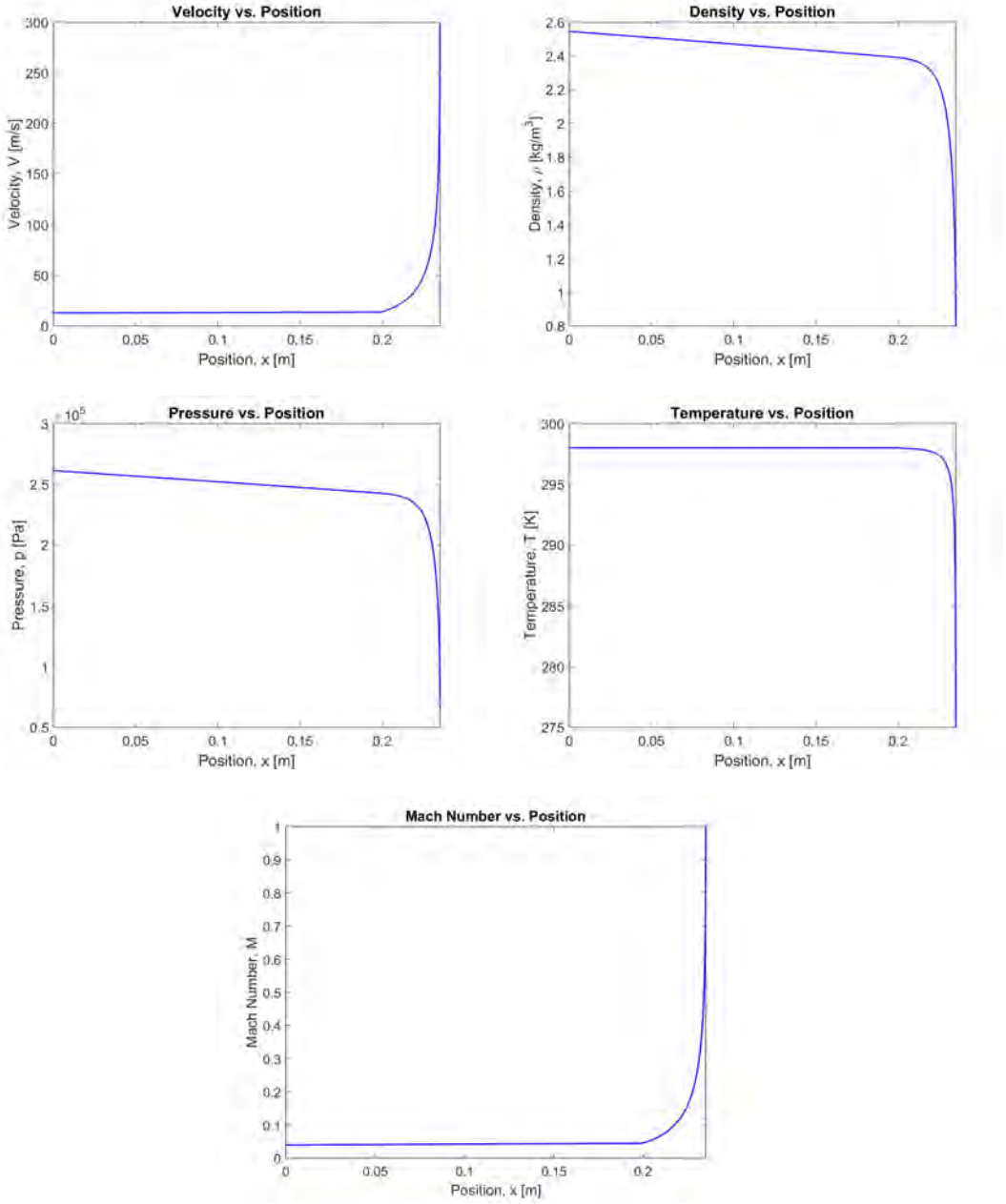

Figure 37: Distribution of the variables V, ρ, p, T and Mach Number over the position considering the change in Area and the frictional effects when the flow enters at 298 K and 12.885 m/s.

The previous graphs show the result of applying the iteration to obtain the suitable conditions for reaching sonic conditions at the exit of the nozzle. As it can be observed, the pressure and the density decrease linearly as the flow goes through the propellant block. Still, the temperature remains constant in this section since any effect considering the addition of heat is included in this part.

5.5.3 Change in Area and Mass Addition

Immediately, the case in which only the changes in area and the addition of mass from the walls is going to be analyzed. The procedure is going to be the same: the calculations are going to be performed in the same conditions as in the first case (only area affects, inlet temperature of 298 K, inlet pressure of 3 bar and inlet velocity of 24.65 m/s), and then the procedure will be iterated until the desired initial conditions that gives us sonic conditions at the exit are found.

In this case the solution is:

$$V = 0.00828 m/s$$
$$p = 1.874 bar$$

As it can be noticed, the velocity has to be decreased much more than in the previous case. This is because the contribution of the mass flow in the equations that are being integrated is much higher than the one offered by the friction forces, which appear only in a single term in two of the equations.

Due to this high contribution, the sonic region is significantly displaced to the inlet part, so a higher variation in the initial conditions must be done to compensate this effects and to finally obtain the desired performance.
the flow is going to be performed in the same conditions as the first case (only area effects, inlet temperature of 298 K, inlet velocity of 26 m/s) and the changes with respect to it are going to be interpreted.

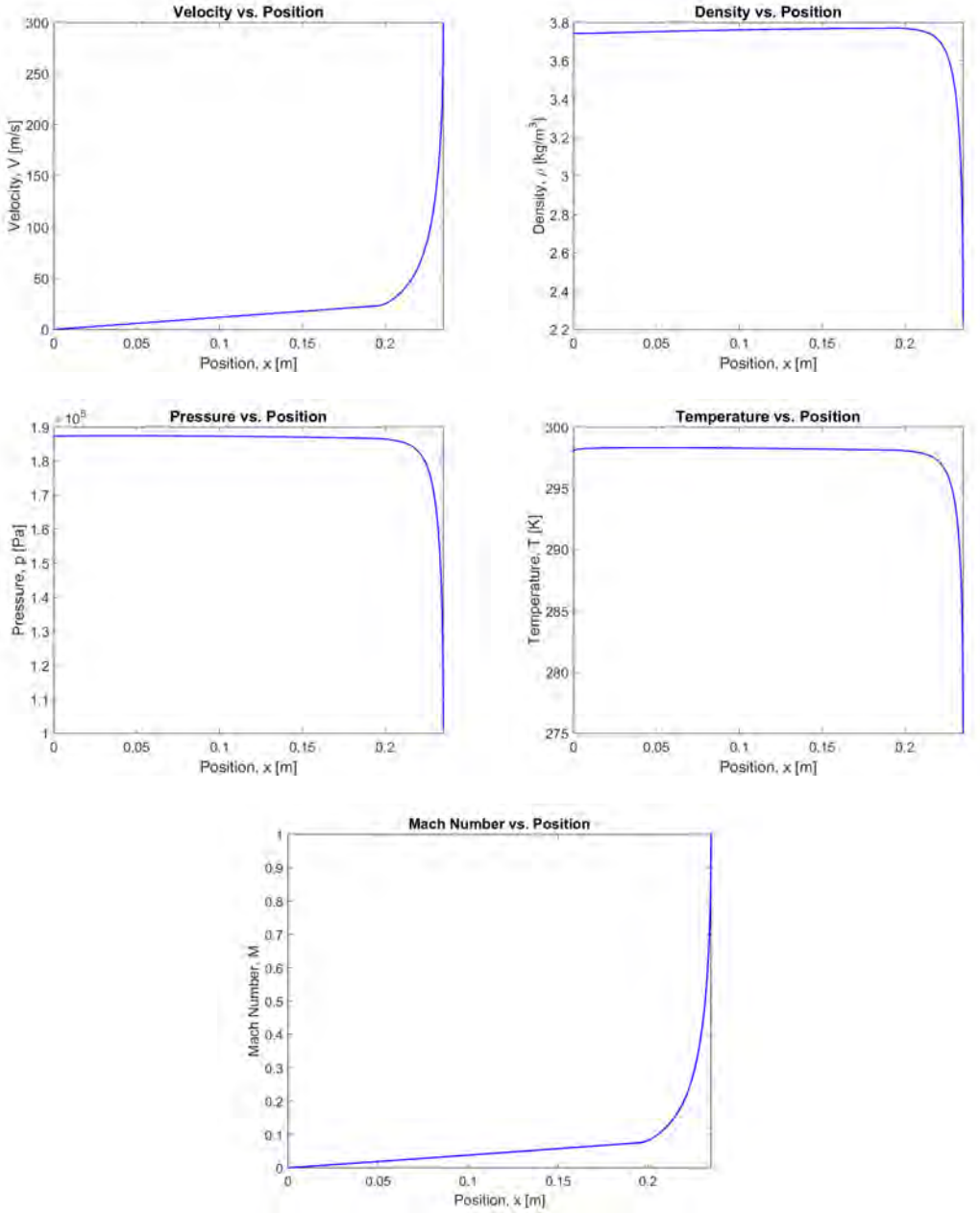

Figure 38: Distribution of the variables V, ρ, p and T over the position considering the change in Area and the mass addition from the walls when the flow enters at 298 K.

As in the previous case, the variation of the properties is weak along the propellant tube and it increases or decreases exponentially in the nozzle part. The temperature is still constant in the propellant tube since the addition of heat is not being considered yet.

5.5.4 General Case

In this last case all the effects are considered: change in area, heat and mass addition ans rejection from and to the walls and frictional effects.

As it could be expected, the addition of all the effects causes a further displacement of the sonic area upstream. This is traduced in a higher necessity in compensating this consequence by changing even more the inlet conditions.
After several iterations, it was obtained that the required initial velocity and pressure to reach sonic conditions in the final section would be:

$$V = 0.001788 m/s$$
$$p = 1.628 bar$$

The distribution of all the properties for this case is shown below:

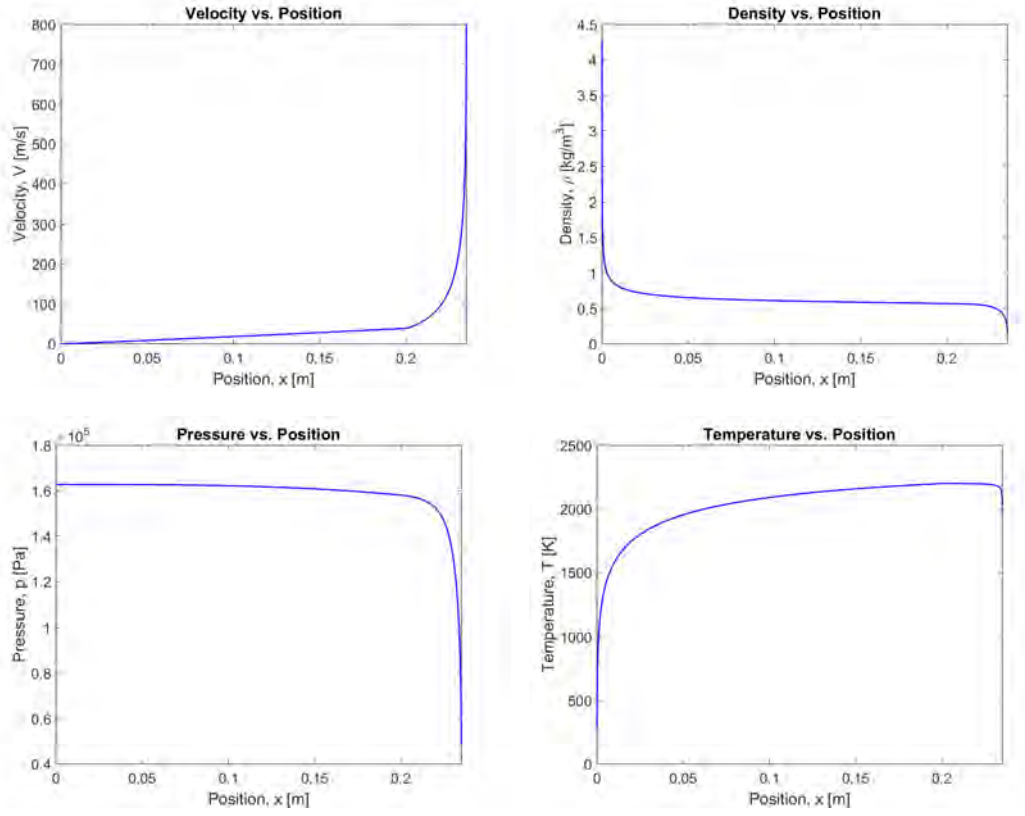

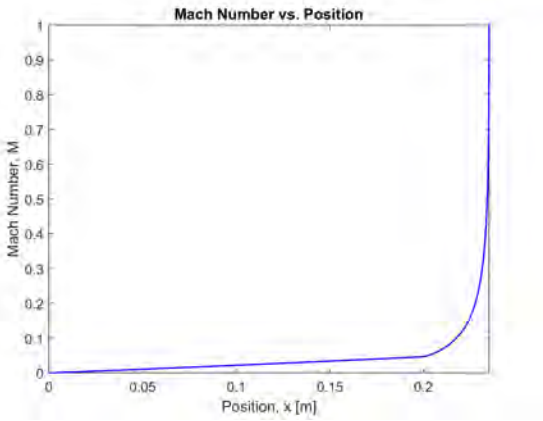

Figure 39: Distribution of the variables V, ρ, p and T over the position for a general case where all the effects are considered.

As it can be observed in the graphs, the variation of all the properties in this general case is higher than in the previous cases:

The velocity increases slightly as the flow passes through the propellant tube and at the point where the contraction of the nozzle starts it increases rapidly until a value that equals M=1.

On the other hand, the density decreases rapidly in the first part of the duct and then it remains almost constant until the end of the nozzle.

The pressure, however, decreases slowly in the propellant tube until, in the nozzle part, it suffers from an abrupt decrease.

Finally, the temperature is the one that changes the most compared to the previous cases, since in this last general case the addition and rejection of heat from and to the walls is being considered. As it can be observed, it increases exponentially during the first part and then it continues rising slowly until it reaches a maximum that corresponds approximately with the adiabatic flame temperature of the PMMA (2470 K).

5.6 Discussion of the mathematical model

From the cases analyzed above it can be conclude that considering effects such as the heat and mass addition or the frictional effects provokes a significant displacement of the sonic section towards the entrance of the duct. In order to compensate it, it is necessary to iterate the calculations until the initial conditions are adjusted to those that give exit Mach number equal to unity. To do it, the velocity is changed to the desired value and then the rest of the properties are calculated from this result.

Also, it has been observed that the more effects being considered, the higher is the shift of the sonic region upstream and the higher changes in the inlet conditions are needed.
Even though the model could have been used to compute the thrust given by the rocket, since all the data necessary to do it is known, it has not been done since the interest of making these calculations would be comparing them to the results obtained from the experimental tests. Nevertheless, at it was already said, due to the problems associated to the load cell it was not possible to obtain feasible results of the thrust provided by the rocket, so there is no possibility of comparing the analytic and experimental results anymore.

6 Conclusions and future work

The present work describes the construction of an upgraded hybrid rocket and the development of a one-dimensional mathematical model that describes its behavior.

As it has been explained, the whole rocket has been redesigned in order to provide a new injection system to make it safer and a renewed thrust measurement system.

Concerning the injection system, further improvements have been made, since now three different gases can be introduced on the rocket. This allows a wider range of experiments that can be achieved by changing the proportion in which the gases are combined or even the gases that we want to use for the experiment.

However, the current gas installation does not allow a good control of the pressure at which the gases are injected, so that it is difficult to predict the mass flow rate of gases going into the hybrid rocket model. This is one of the parts that is going to remain as an objective for further improvements in the project since this improvement would lead to better measurements and calculations of the performance of the rocket.

Also, a new ignition system which consists of a glow plug installed in the upper part of the rocket was made. The glow plug is powered by applying some voltage to it, and when its igniting head gets in contact with the gases, the combustion starts. Thanks to this new system, the previous method used to ignited the rocket (a person had to stand in the ignition room and the combustion started when a match was introduced through the exit orifice of the model) has been eliminated, making the model safer.

The last main objective of the project concerning the geometry of the rocket model was the installation of a new thrust measurement system which consists on a load cell placed upstream, in contact with the external face of the thruster. However, it was not possible to obtain feasible measurements from this system since the outputs coming from the cell would not give any information (the output voltage during the ignition was almost the same as the one given when the rocket is at rest).

For this reason, the improving of this system is going to remain as an important objective for the future work. Also, a new acquisition data can be created by programming a DAQ system that automatically traduces the output voltage into a force so that the thrust produced by the rocket can be known immediately without needing intermediate computations.

The second part of the project consisted on the implementation of a one-dimensional mathematical model to predict the behavior of the rocket. The four equations that give us the characteristics of the flow (mass conservation equation, momentum equation, energy equation and the equation of state) were integrated with Matlab, so that the properties of the flow (temperature, velocity, pressure and density) could be known at any point of the duct.

Reasonable results have been obtained from it, and thanks to the model, the performance of the rocket can be known. However, the model can still be improved by making a two-dimensional model that simulates better the real performance of the rocket.

Also the hypotheses that have been made to establish the inputs of the model can be further developed to obtain more realistic results, so that the analytic results are as similar to the real behavior of the rocket as possible.

In future projects, combining the improvements related to the mechanical part and the ones concerning the mathematical model, the measurements taken from both methods can be compared and studied.

7 Cost analysis of work done

The budget for this project is the following:

Equipment Cost

Product Description	Unitary Cost	Number of Units	Total Cost
Grooving Tool	39.93 €	2	79.86 €
Annular Broach for Steel	119.55 €	1	119.55 €
Inox Bar 1.4307	3.612 €/Kg + 45.254 €	62.6	271.35 €
Glow Plug Tap	70.66 €	1	70.66 €
Glow Plugs	6 €	5	30 €
Load Cell	84.87 €	1	84.87 €
		Subtotal	656.29 €

Table 13: Budget of the Equipment

Personnel Cost

Approximate cost per hour	**Days of work**	**Work-hours**	**Total Cost**
41 €/h	11 days	3 hrs/day	1353 €

Table 14: Budget of the Personnel

The total budget for the project is **2009.29 €**

References

[1] George P. Sutton, Oscar Biblarz *Rocket Propulsion Elements, 8th Edition.* John Wiley and Sons, Hoboken, New Jersey, 2010.

[2] Space Propulsion Group, Inc.
`http://www.spg-corp.com/space-propulsion-group-resources.html`

[3] Walter E. Hammond. *Design Methodologies for Space Transportation System.* American Institute of Aeronautics and Astronautics AIAA Education Series, Reston, Virginia, 1947.

[4] A. Karabeyoglu. *Advanced Rocket Propulsion Course Lecture 10: Hybrid Rocket Propulsion Design Issues.* Department of Aeronautics and Astronautics, Stanford University, 2012.

[5] B. Geneviève, Michael J. Brooks, Jean-François P. Pitot de la Beaujardiere, Lance W. Roberts. *Performance Modeling of a Paraffin Wax / Nitrous Oxide Hybrid Rocket Motor.* 49th AIAA Aerospace Sciences Meeting including the New Horizons Forum and Aerospace Exposition, Orlando, Florida, 2011.

[6] Pierre-Jean Bristeau, Nicolas Petit. *Trajectory estimation for a hybrid rocket.* Centre Automatique et Systèmes, Unité Mathématiques et Systèmes, Mines ParisTech, Paris, France. AIAA Guidance, Navigation and Control Conference, 10-13 August 2009, Chicago, Illinois.

[7] Stephen R. Turns *An introduction to combustion : concepts and applications, 3rd Edition.* McGraw Hill, New York, 2011.

[8] Ascher H. Shapiro *The Dynamics and Thermodynamics of Compressible Fluid Flow, Vol I.* The Ronald Press Company, New York, 1953.

[9] Ascher H. Shapiro *The Dynamics and Thermodynamics of Compressible Fluid Flow, Vol II.* The Ronald Press Company, New York, 1954.

[10] W. R. Zeng, S.F. Li, W.K. Chow *Review on Chemical Reactions of Burning Poly(methyl methacrylate) PMMA*. Journal of Fire Sciences, Vol 20, September 2002.

[11] V. Mittal. *Functional Polymer Blends: Synthesis, Properties, and Performance, 0th Edition* CRC Press, Taylor & Francis Group, 2012.

[12] Matbase:
`http://www.matbase.com/material-categories/natural-and-synthetic-polymers/commodity-polymers/material-properties-of-polymethyl-methacrylate-extruded-acrylic-pmma.html#manufacturing-properties`

[13] Brian T. Rhodes. *Burning Rate and Flame Heat Flux for PMMA in the Cone Calorimeter.* University of Maryland, May 1994.

[14] National Institute of Standards and Technology, NIST.
`http://webbook.nist.gov/cgi/cbook.cgi?Source=1952ERD%2FJGE770&Units=&Mask=28F`

[15] Pedro P. de Oliveira Alcarria Guerreiro. *Preliminary Study of a Hybrid Rocket.* Master of Science Degree in Mechanical Engineering, Instituto Superior Técnico Lisboa, May 2013.

[16] Mohamad Khattab. *Innovative Solid Fuels for Hybrid Rocket Propulsion.* Corso di Laurea Specialistica in Ingegneria Aeronautica, Facoltà di Ingegneria Industriale, Politecnico Di Milano, 2010-2011.

[17] G. J. Van Wylen, R. E. Sonntag. *Fundamentals of Classical Thermodynamics, 2nd Edition.* John Wiley and Sons, 1978.

[18] Christopher E. Brennen. *Fundamentals of Multiphase Flows.* California Institute of Technology Pasadena, Cambridge University Press, California, 2005.

[19] Francesco Barato. *Numerical and Experimental Investigation of Hybrid Rocket Motors Transient Behavior.* Scuola di Dottorato di Ricerca in Scienze Tecnologie e Misure Spaziali Indirizzo di Astronautica e Scienze da Satellite, Universita Degli Studi di Padova, January 2013.

[20] Tomasso Astarita. *Corso di Complimenti di Gasdinamica.* Università degli Studi di Napoli Federico II, Napoli, 2014.
`www.docenti.unina.it`

[21] Maurice J. Zucrow, Joe D. Hoffman. *Gas Dynamics, Vol I.* John Wiley and Sons, 1976.

[22] Maurice J. Zucrow, Joe D. Hoffman. *Gas Dynamics, Vol II.* John Wiley and Sons, 1976.

[23] Altman, D., A. Holzman, *Overview and History of Hybrid Rocket Propulsion, Fundamentals of Hybrid Rocket Combustion and Propulsion, Vol. 218, Edited by M. J. Chiaverini, and K. K. Kuo.* Progress in Astronautics and Aeronautics, AIAA, Reston, VA, 2007.

[24] *American National Standards Letter Symbols for Rocket Propulsion.* ASME Publications, 1959.

[25] P. G. Hill, C. R. Peterson, *Mechanics and Thermodynamics of Propulsion.* Addison-Wesley, Reading, Massachusetts, 1992.

[26] H. R. Lips. *Experimental Investigation of Hybrid Rocket Engines Using Highly Aluminized Fuels.* Journal of Spacecraft and Rockets, Vol. 12, No. 9, 1999.

[27] Delft University of Technology:
`http://www.lr.tudelft.nl/en/organisation/departments/space-engineering/space-systems-engineering/expertise-areas/space-propulsion/design-of-elements/rocket-propellants/thermal/`

[28] Greg Zilliac. *Hybrid Rocket Propulsion: Past, Present, and Future.*Presentation, November 2010.

[29] Air Liquide:
`http://encyclopedia.airliquide.com/encyclopedia.asp?GasID=26&LanguageID=9&CountryID=19`

[30] The Engineering Toolbox:
`http://www.engineeringtoolbox.com/`

[31] M. A. Karabeyoglu, D. Altman, D. Bershader. *Transient Combustion in Hybris Rockets* 31st AIAA Joint Propulsion Conference, San Diego, California, 1995.

[32] B. Greiner, R. Federick. *Results of Labscale Hybrid Rocket Motor Investigation, Paper 92-3301.* 28th AIAA Propulsion Conference and Exhibit, Nashville, Tennessee, 1992.

[33] G. Zilliac, M. A. Karabeyoglu. *Hybrid Rocket Fuel Regression Rate Data and Modeling.* 42nd AIAA Joint Propulsion Conference and Exhibit, Sacramento, California, 2006.

[34] R. C. Reid, J. M. Prausnitz, T. K. Sherwood. *The Properties of Gases and Liquids, 3rd Edition.* McGraw-Hill, New York, 1977.

[35] C. Huggett. *Estimation of Rate of Heat Release by Means of Oxygen Consumption Measurements.* Fire and Materials, 4(2): 61-65, 1980.

[36] Richard Nakka's Experimental Rocketry Web Site:
`http://www.nakka-rocketry.net/burnrate.html`

[37] Altman, A. Holzman. *Fundamentals of Hybrid Rocket Combustion and Propulsion, Vol. 218, Progress in Astronautics and Aeronautics.* AIAA, Reston, Virginia, 2001.

[38] Web QC, Chemical Portal
http://www.webqc.org/mmcalc.php

[39] Electronics
https://electronicspani.com/voltage-source-and-current-source/

[40] Isaac T. Leventon, *Evolution of Flame to Surface Heat Flux During Upward Flame Spread on Polymethyl Methacrylate (PMMA).* Graduate School of the University of Maryland, Master of Science, 2011.

Annex I: Part 1 - Plan

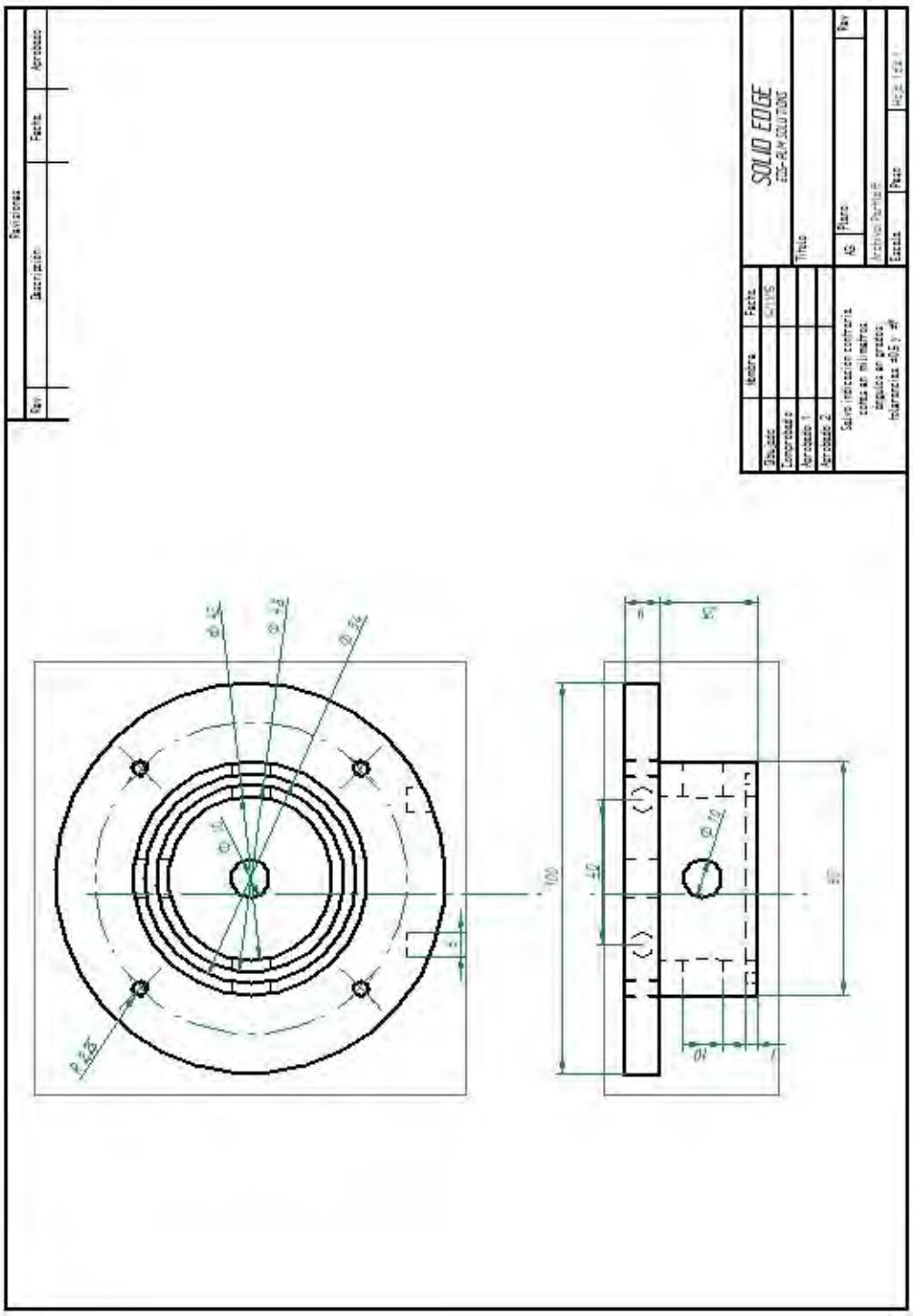

Annex II: Part 2 - Plan

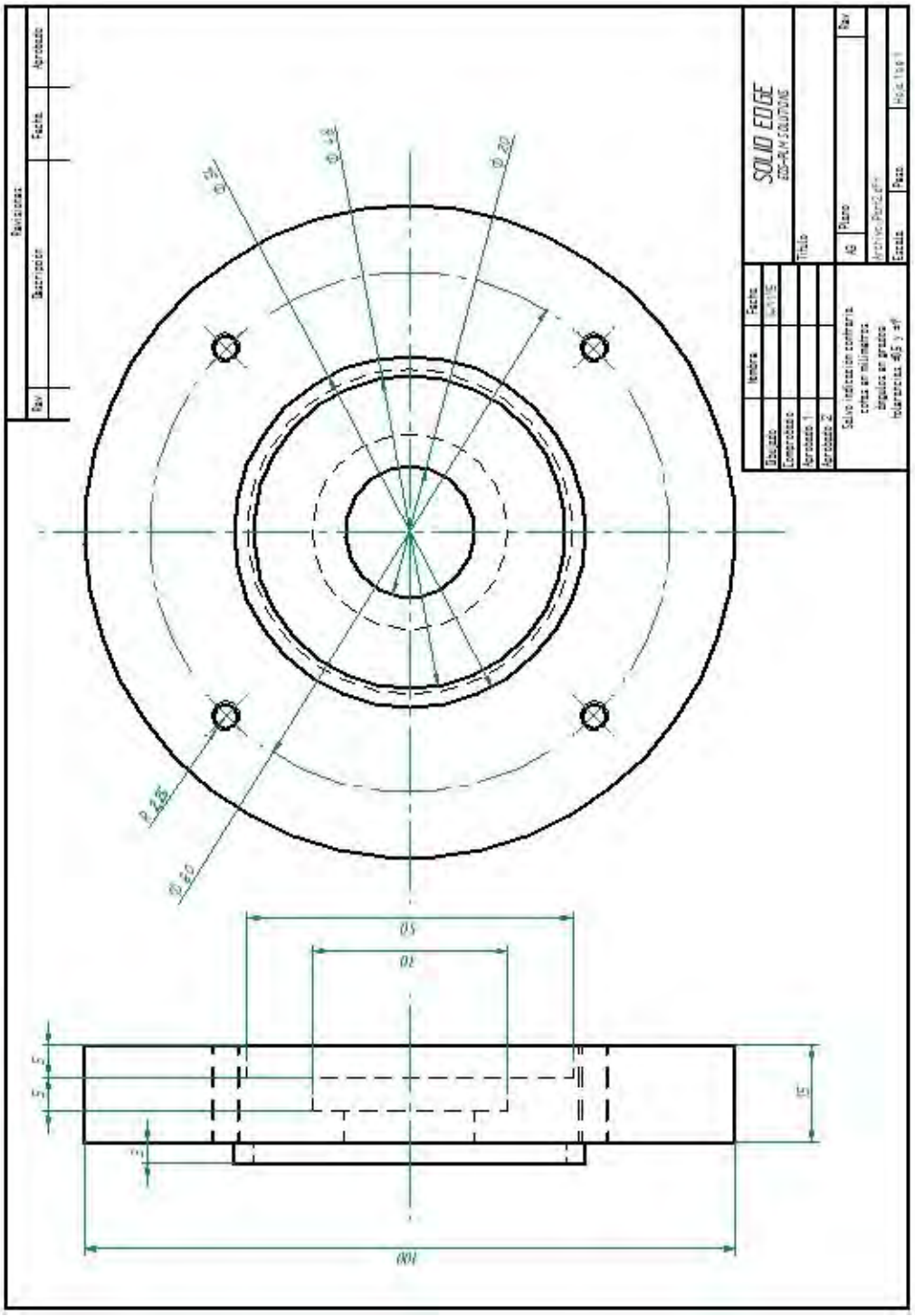

Annex III: Part 3 - Plan

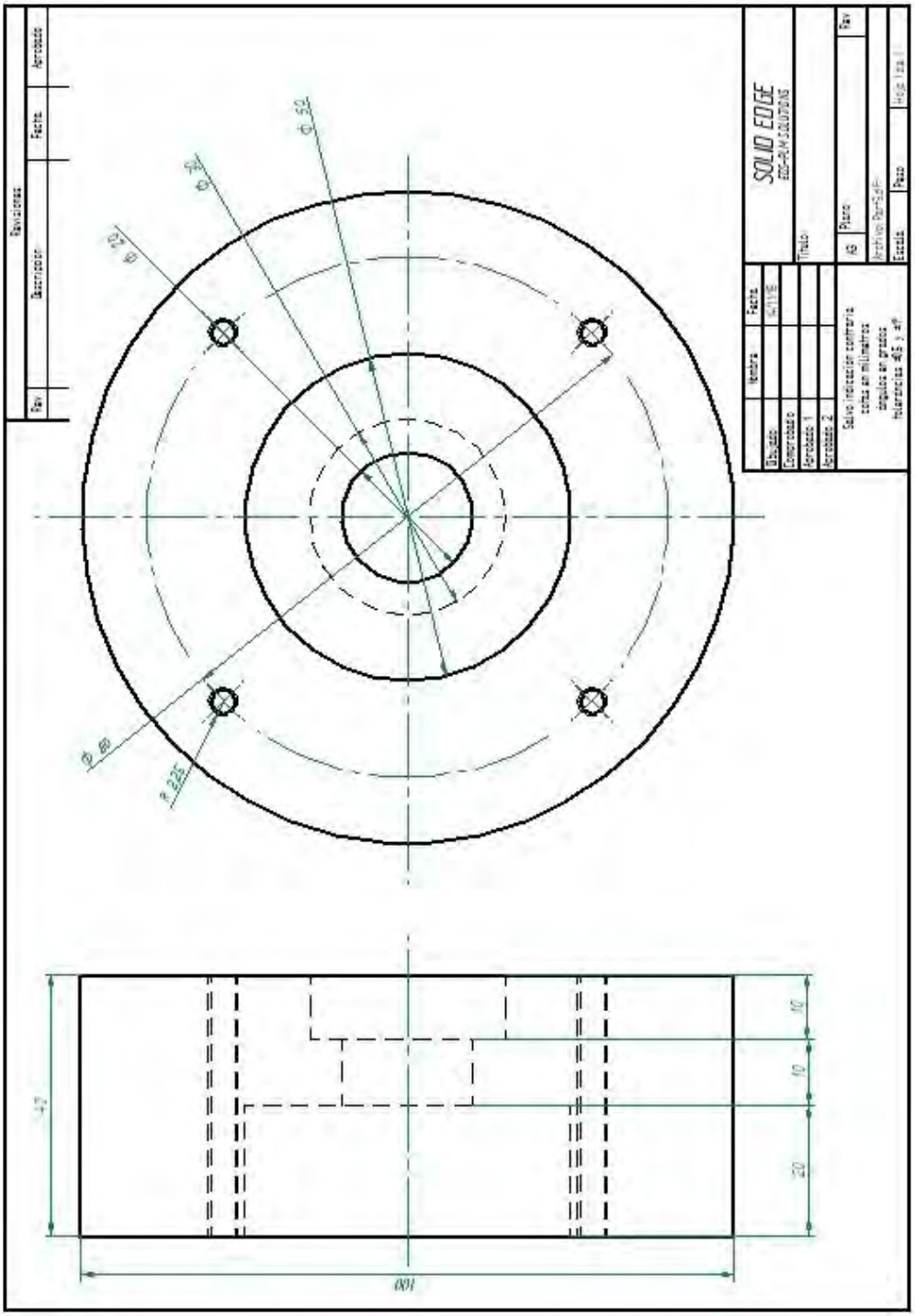

Annex IV: Part 4 - Plan

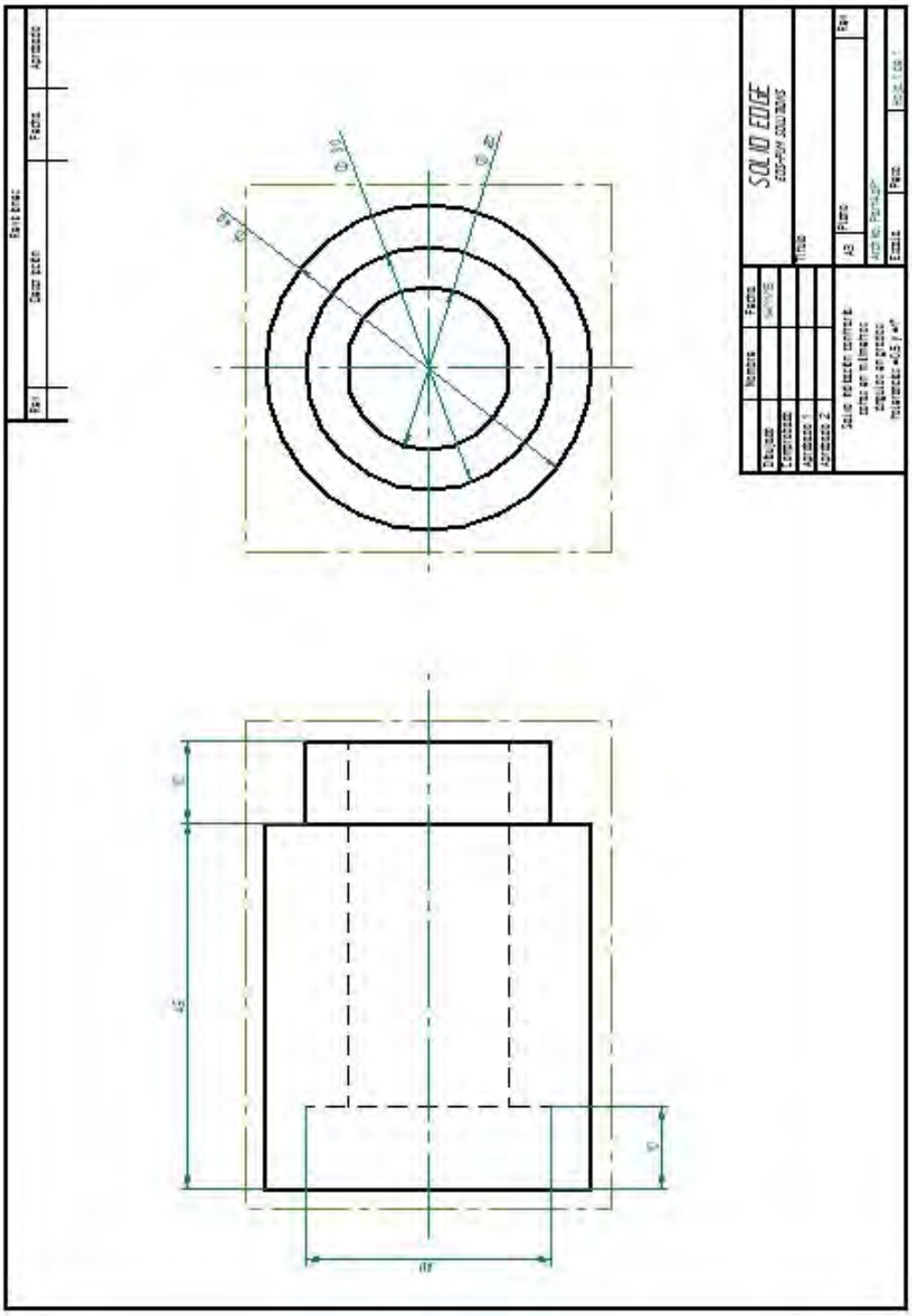

Annex V: Part 5 - Plan

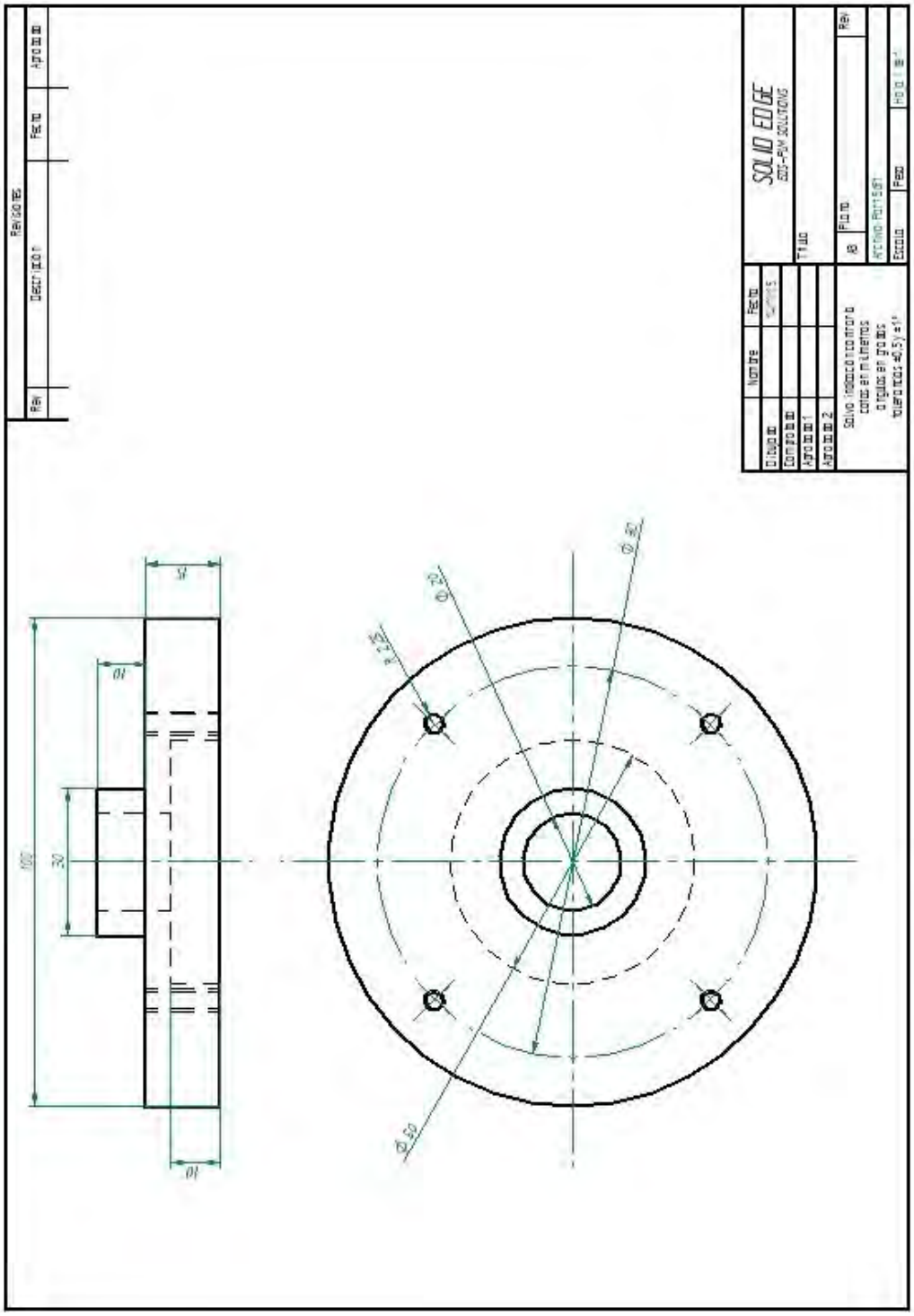

Annex VI: Part 6 - Plan

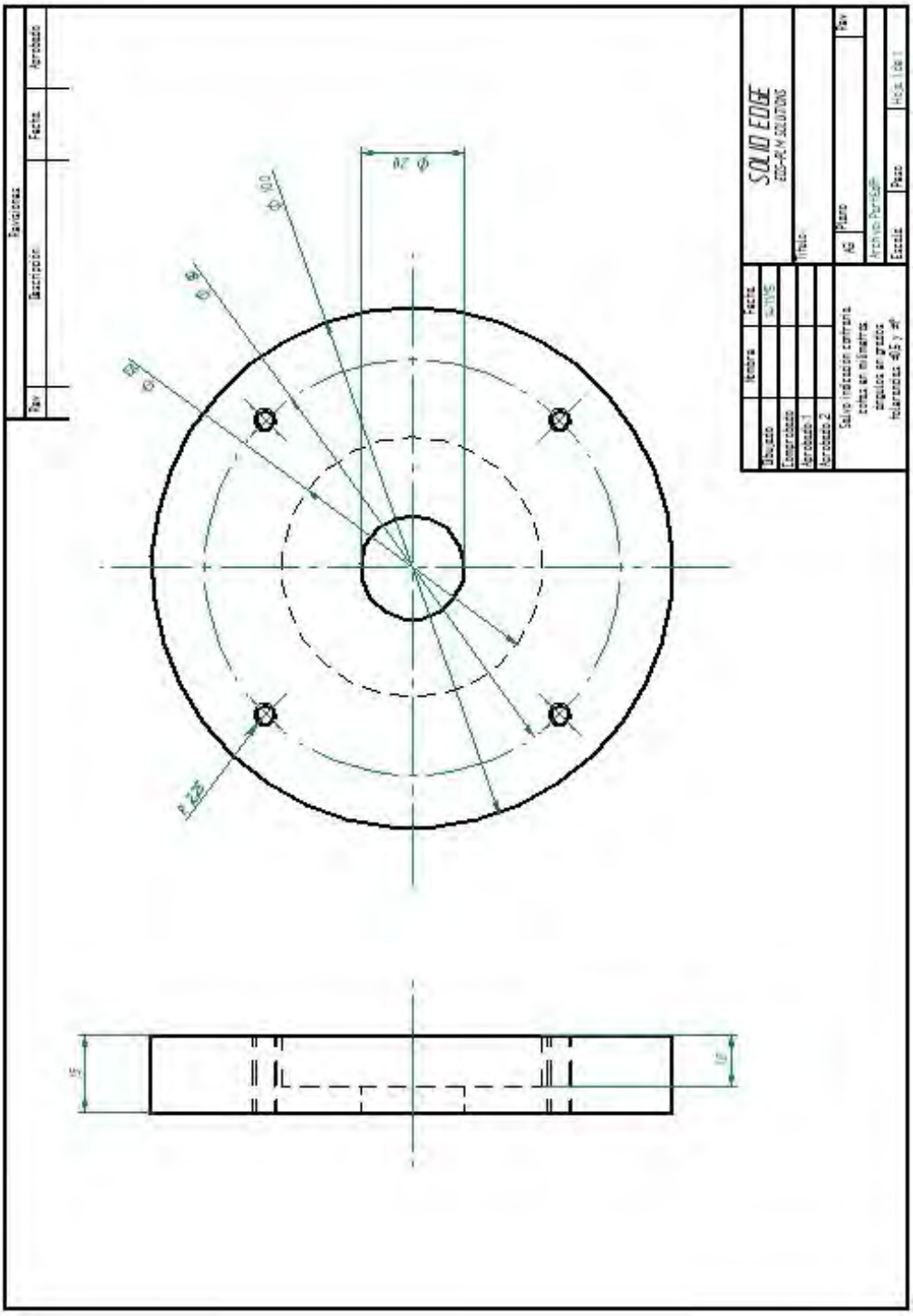

Annex VII: Graphite Mouthpiece - Plan

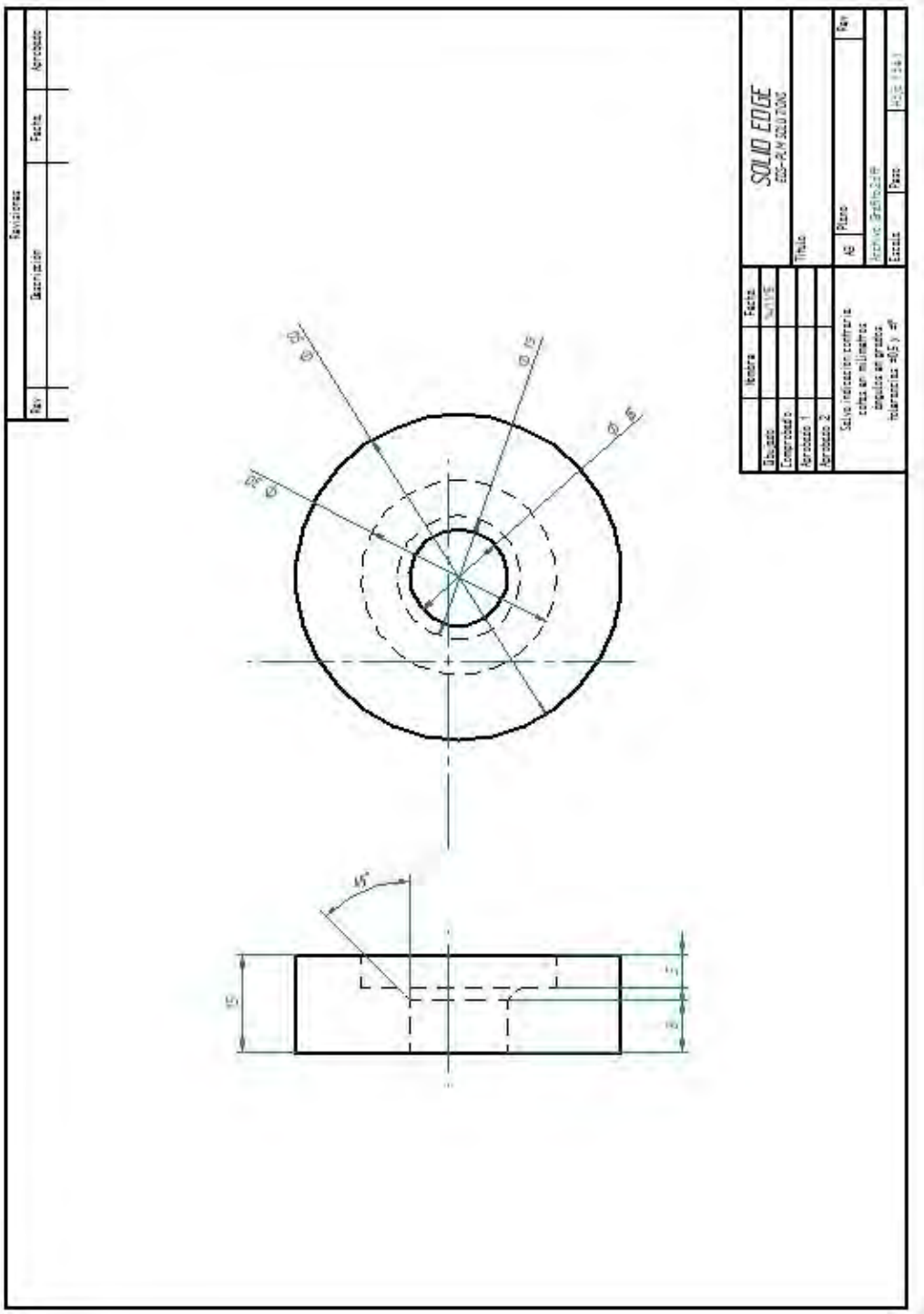

Annex VIII: Graphite Nozzle - Plan

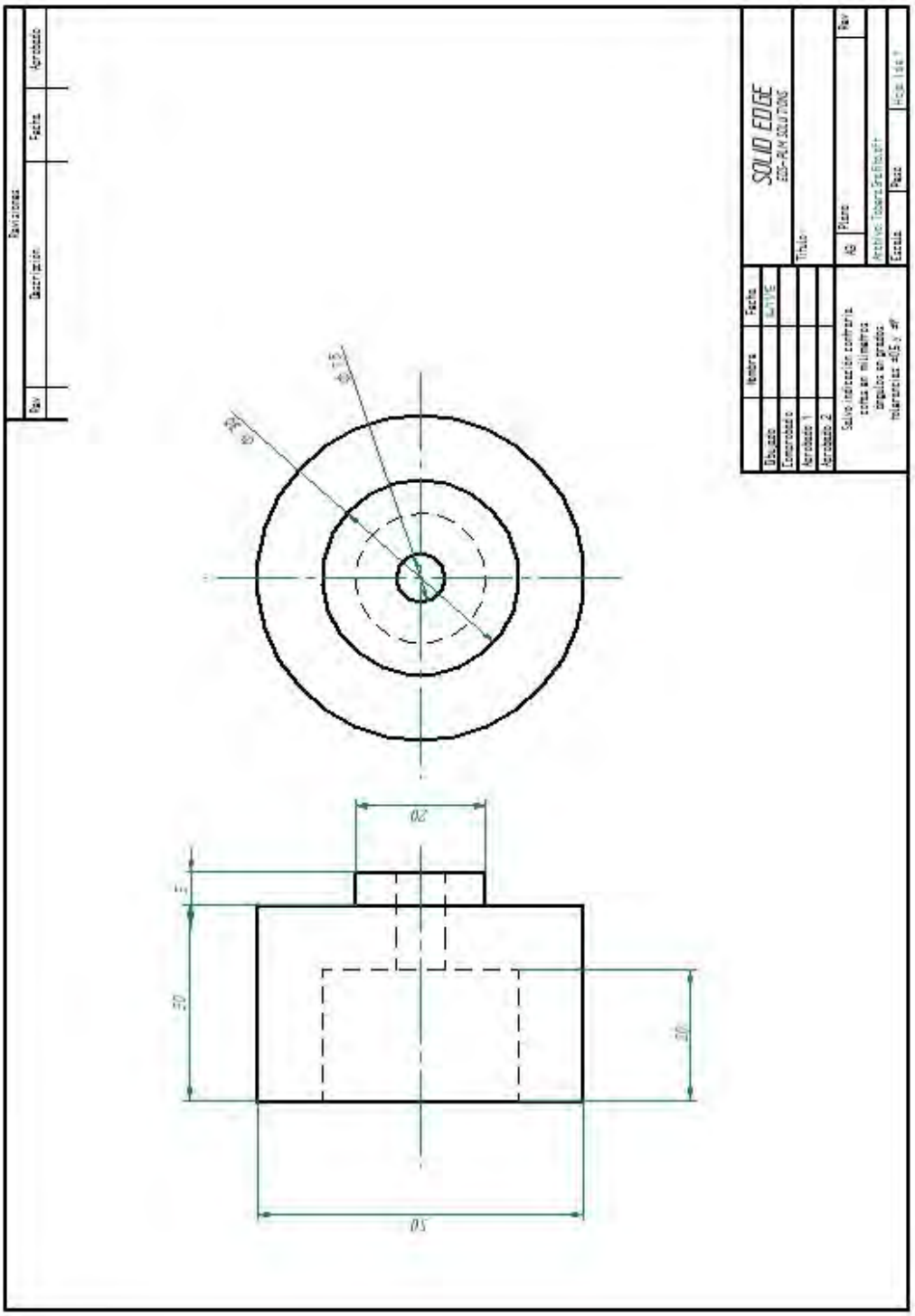

Annex IX: Load Cell User Guide

measurement SPECIALTIES™

FC22 Compression Load Cell

- **10 – 100 lbf Ranges**
- **High Level or mV Outputs**
- **Interchangeable**
- **Compact Easy to Fixture Design**
- **CE Compliance**

RoHS CE

DESCRIPTION

The FC22 is a medium compression force sensor that creates new markets previously unrealizable due to cost and performance constraints. The FC22 offers normalized zero and span for interchangeability and is thermally compensated for changes in zero and span with respect to temperature.

The FC22 incorporates MEAS' proprietary Microfused technology which employs micromachined silicon piezoresistive strain gages fused with high temperature glass to a high performance stainless steel substrate. Microfused technology eliminates age-sensitive organic epoxies used in traditional load cell designs providing excellent long term span and zero stability. The FC22 measures direct force and is therefore not subject to lead-die fatigue failure common with competitive designs which use a pressure capsule embedded within a silicone gel-filled cavity. Operating at very low strains, Microfused technology provides an essentially unlimited cycle life expectancy, superior resolution, and high over-range capabilities.

Cost-optimization of the FC22 brings your OEM product to life whether you need thousands or millions of load cells annually. Although the standard model is ideal for a wide range of applications, our dedicated design team at our Load Cell Engineering Center is ready to provide you with custom designs for your OEM applications.

Please refer to the FS20 for lower force applications or the FC23 for higher force applications.

FEATURES

- Small Size
- Low Noise
- Robust: High Over-Range Capability
- High Reliability
- Low Deflection
- Essentially Unlimited Cycle Life Expectancy
- Low Off Center Errors
- Fast Response Time
- 10 to 100 lbf Ranges
- Reverse Polarity Protected

APPLICATIONS

- Medical Infusion Pumps
- Robotics End-Effectors
- Variable Force Control
- Load and Compression Sensing
- Exercise Machines
- Pumps
- Contact Sensing
- Weighing
- Household Appliances

FC22 Compression Load Cell

STANDARD RANGES

Range	lbf
0 to 10	•
0 to 25	•
0 to 50	•
0 to 100	•

PERFORMANCE SPECIFICATIONS

Supply Voltage: 5.0V, Ambient Temperature: 25°C (unless otherwise specified)

PARAMETERS	MIN	TYP	MAX	UNITS	NOTES
Span (Unamplified)	19	20	21	mV/V	1
Span (Amplified)	3.88	4.00	4.12	V	1
Zero Force Output (Unamplified)	-1	0	1	mV/V	1
Zero Force Output (Amplified)	0.3	0.5	0.7	V	1
Accuracy (non linearity, hysteresis, and repeatability)		±1		%Span	2
Output Resistance (Unamplified)		2.2		kΩ	
Input Resistance (Unamplified)		3		kΩ	
Temperature Error – Zero	-1.25		1.25	%Span	3
Temperature Error – Span	-1.25		1.25	%Span	3
Long Term Stability (1 year)		±1		%Span	
Maximum Overload			2.5X	Rated	
Compensated Temperature	0		50	°C	
Operating Temperature	-40		+85	°C	
Storage Temperature	-40		+85	°C	
Excitation Voltage (Unamplified)			5	Vdc	
Excitation Voltage (Amplified)	3.3		5	Vdc	
Isolation Resistance (250Vdc)	50			MΩ	
Deflection at Rated Load			0.05	mm	
Humidity	0		90	%RH	
Weight		18.41		grams	

For custom configurations, consult factory.

Notes
1. Ratiometric to supply.
2. Best fit straight line.
3. Maximum temperature error over compensated range with respect to 25°C.

CE Compliance

IEC61000-4-2 (4 kV/ 4kV (Air/Contact))
IEC61000-4-3 (3 V/m)
IEC55022 Class A

FC22 Compression Load Cell

DIMENSIONS

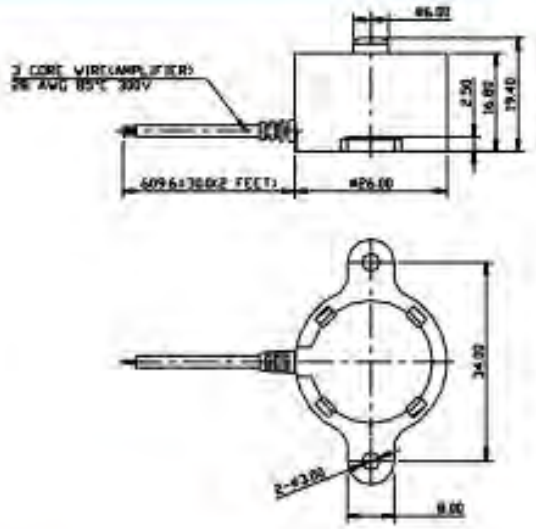

CONNECTIONS

Millivolt Bridge Version

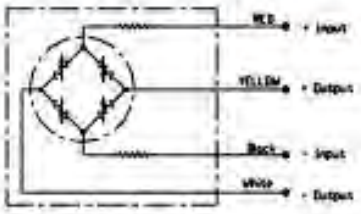

High Level Amplified Output

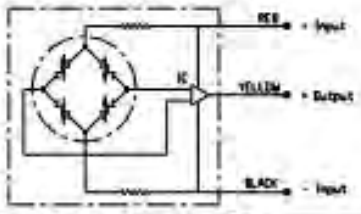

FC22 Compression Load Cell

ORDERING INFORMATION

FC22	3	-	1	0000	-	0010	-	L
Model	**Output**	-	**Connection**	**Specials**	-	**Force Range (lbf)**	**Multiplier**	**Units**
FC22	0 = Uncompensated 1 = 20mV 3 = 0.5 – 4.5V	-	1 = 2ft Cable	0000	-	0010 0025 0050 0100	- = None	L = lbf

NORTH AMERICA

Measurement Specialties
45738 Northport Loop West
Fremont, CA 94538
Tel: 1-800-767-1888
Fax: 1-510-498-1578
Sales: pfg.cs.amer@meas-spec.com

EUROPE

Measurement Specialties
(Europe), Ltd.
26 Rue des Dames
78340 Les Clayes-sous-Bois, France
Tel: +33 (0) 130 79 33 00
Fax: +33 (0) 134 81 03 59
Sales: pfg.cs.emea@meas-spec.com

ASIA

Measurement Specialties
(China), Ltd.
No. 26 Langshan Road
Shenzhen High-Tech Park (North)
Nanshan District, Shenzhen 518057
China
Tel: +86 755 3330 5088
Fax: +86 755 3330 5099
Sales: pfg.cs.asia@meas-spec.com

Annex X: Combustion of PMMA

First of all, the temperature is increased by an external heat source to the point where the chemical bonds begin to break, generating monomers[10]. After this, the resulting products undergo combustion. This is the gas-phase oxidation.

Thermal Decomposition

PMMA can be synthesized in two different ways. Depending on this, it can be obtained radically polymerized PMMA of anionically polymerized PMMA.[10]

Radically polymerized PMMA decomposes at a lower temperature, approximately 493 K, since it has unsaturated groups at its ends, which make it more unstable. [14]

On the other side, anionically polymerized PMMA is thermally more stable. It decomposes at 573 K approximately.[10]

Thermally Oxidative Decomposition

The reaction between oxygen and poly(methyl methacrylate) is very complex. Its dynamics and mechanisms depend on many other variables apart from the nature of the components, like the physical characteristics of the surroundings, the heating source and the position and size of the particles.

In contact with oxygen, PMMA goes through a thermal oxidative decomposition that is a consequence of the reaction of the oxygen with macro-radicals, forming hydro-peroxides which are very unstable and decompose quickly into free radicals. However, the main product of this decomposition is MMA, the monomer of PMMA. [10]

This decomposition occurs at approximately 533 K and involves the following steps:

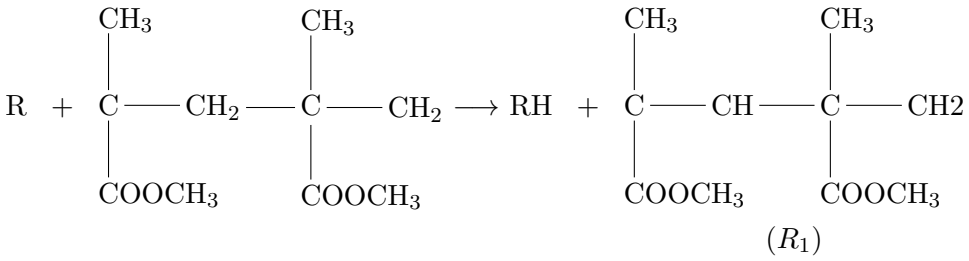

Where R is a free radical that acts as an initiator.

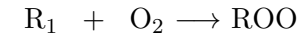

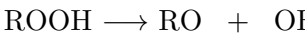

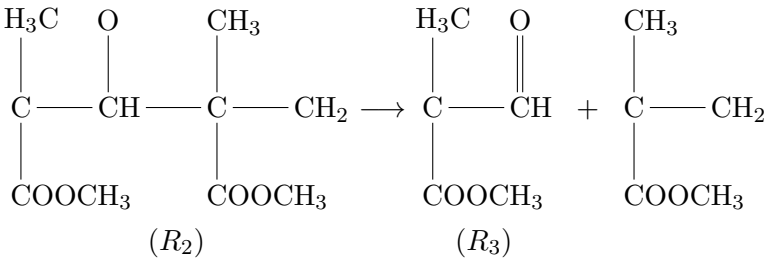

The next step is the decomposition of radical R_3:

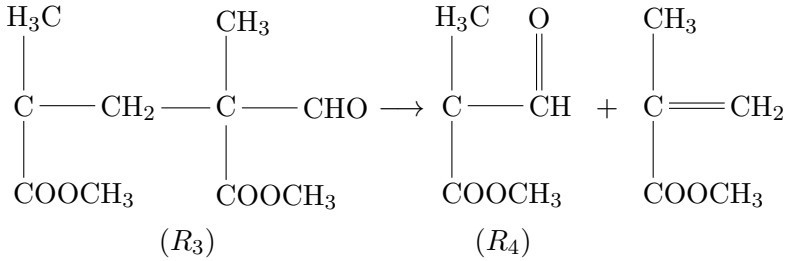

By rearrangement of the radical 4 with H, 2-methyl-oxirane carbonic acid methyl ester is generated:

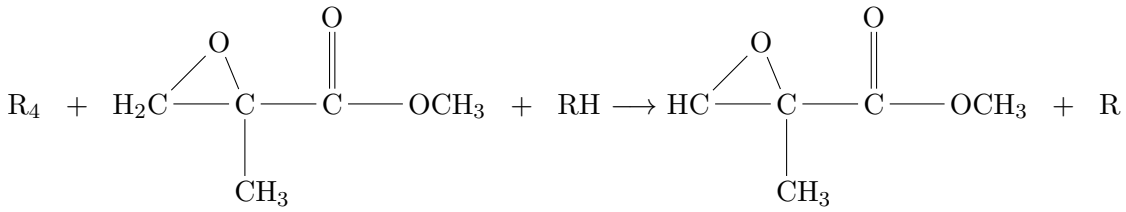

(I)

The next steps consist on the generation of methyl piruvate (II):

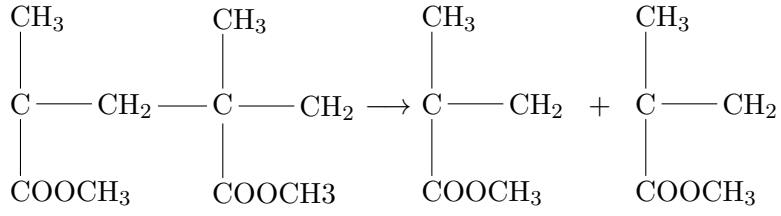

(R_5) (R_6)

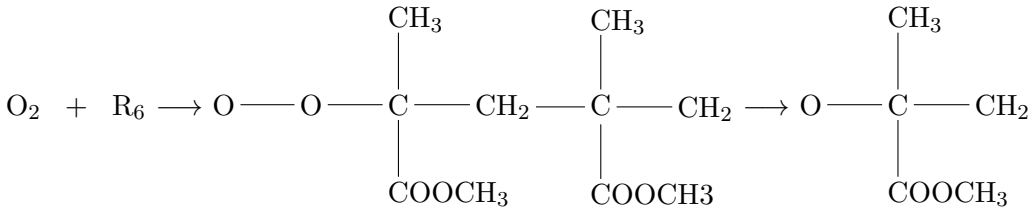

(R_7) (R_8)

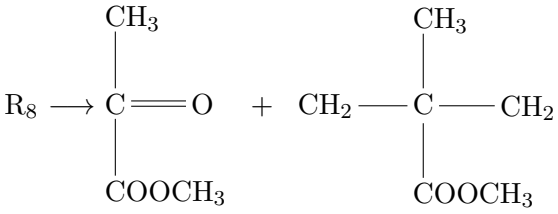

(II)

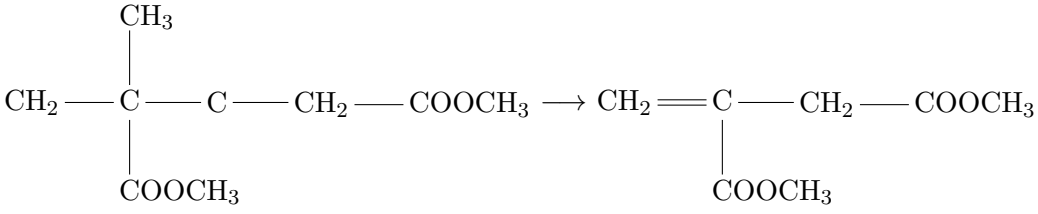

(III)

Te stabilizing effect of the oxygen is shown in the following reaction:

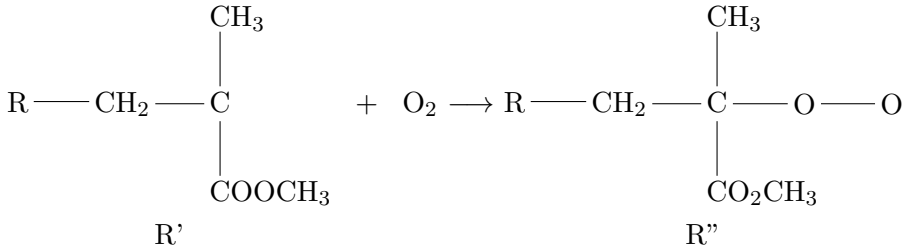

The radical R", due to its thermally stability, inhibits the decomposition of PMMA.

As it can be observed in the reactions above, the decomposition of the radical R_4 will lead to the formation of 2-Methyl-oxirane carbonic acid methyl ester. In the following step, methyl piruvate will be produced, while the radical R_8 will generate methyl pyruvate[10].

At a low temperature, oxygen will act as an stabilizer in the reaction. Nevertheless, it will intensify random scissions and it will increase the rate of decomposition at higher temperatures.

Decomposition of Monomer MMA

As it was already said, MMA is the main product of the decomposition of poly(methyl methacrylate). This monomer, as the reaction continues, will decompose into smaller products that can undergo combustion.

This gas-phase process involves two rupture paths: one of them consists of the C-O bond breaking reaction, and the other one corresponds to decarboxylations.

The decomposition process of MMA combined with oxygen leads to the formation of CH_3OH, CH_4, 2-methyl propylene, propylene, formaldehyde, methyl pyruvate and acetone. The reaction mechanisms are the following:

First, the monomer MMA decomposes into the radicals R_1 and R_2

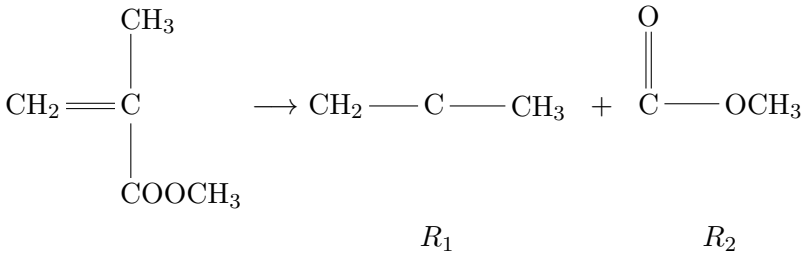

Then R_2 continues to break to give carbon dioxide and carbon monoxide:

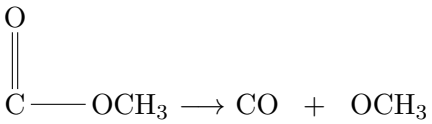

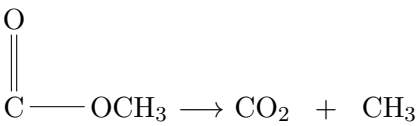

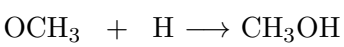

On the other hand, R_1 will react with H and methyl to produce propylene and 2-methyl propylene respectively:

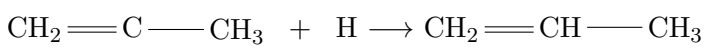

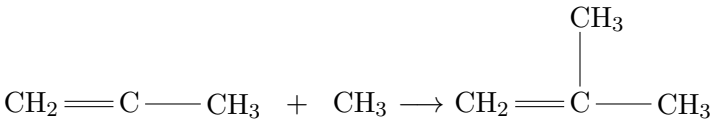

Right after, propylene is combined with oxygen to produce acetone:

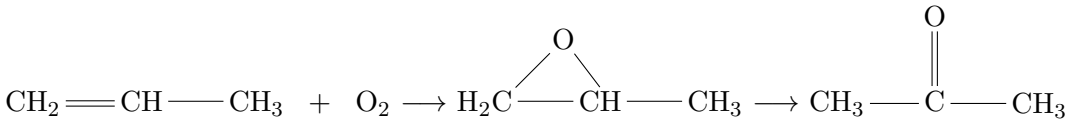

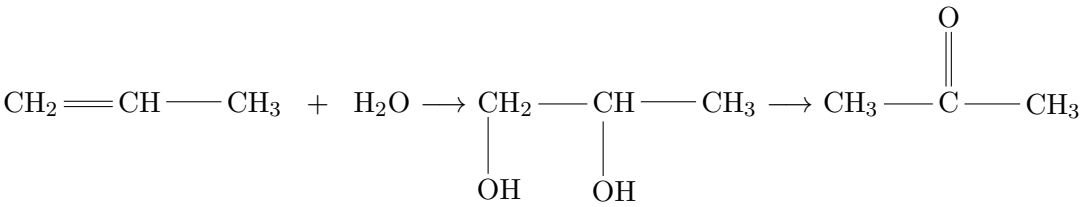

In the last part of the process, methyl pyruvate and formaldehyde will be produced. First, MMA reacts with oxygen to produce the radicals R_3 and R_4, and then these radicals will dehydrate to generate methyl pyruvate and formaldehyde:

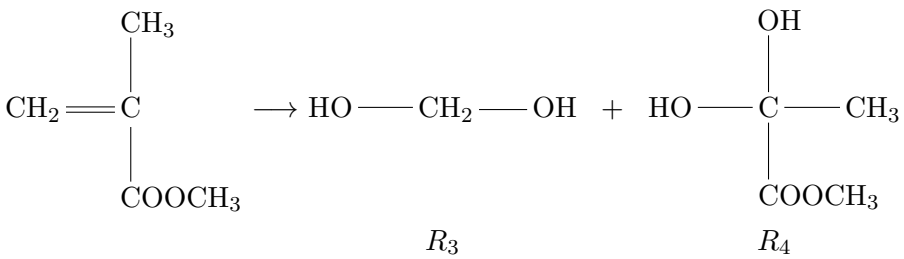

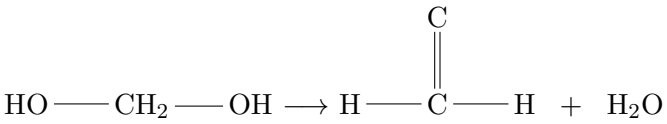

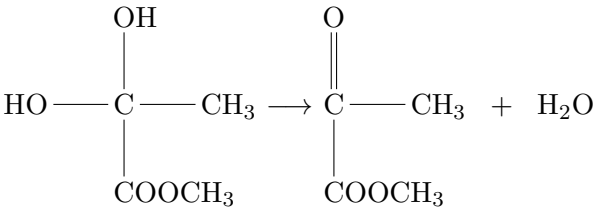

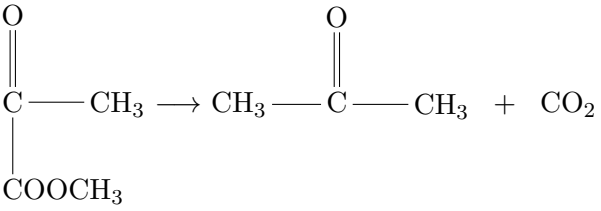

Finally, the reaction of combustion of the small products can be written as:

$$X + O_2 \longrightarrow CO + CO_2 + H_2O$$

Where X corresponds to methane, formaldehyde, methanol, propylene, acetone, etc.